



HAL
open science

Implication de l'oncogène STAT3 dans la réponse aux traitements de chimiothérapies : Application au cancer colorectal

Sandy Courapied

► **To cite this version:**

Sandy Courapied. Implication de l'oncogène STAT3 dans la réponse aux traitements de chimiothérapies : Application au cancer colorectal. Biologie cellulaire. Université d'Angers, 2010. Français. NNT: . tel-00576728

HAL Id: tel-00576728

<https://theses.hal.science/tel-00576728>

Submitted on 15 Mar 2011

HAL is a multi-disciplinary open access archive for the deposit and dissemination of scientific research documents, whether they are published or not. The documents may come from teaching and research institutions in France or abroad, or from public or private research centers.

L'archive ouverte pluridisciplinaire **HAL**, est destinée au dépôt et à la diffusion de documents scientifiques de niveau recherche, publiés ou non, émanant des établissements d'enseignement et de recherche français ou étrangers, des laboratoires publics ou privés.

RESEARCH

Open Access

Regulation of the Aurora-A gene following topoisomerase I inhibition: implication of the Myc transcription Factor

Sandy Courapied^{1†}, Julia Cherier^{1†}, Arnaud Vigneron¹, Marie-Bérangère Troadec³, Sandrine Giraud⁴, Isabelle Valo², Claude Prigent³, Erick Gamelin¹, Olivier Coqueret^{1*†}, Benjamin Barré^{1*†}

Abstract

During the G2 phase of the cell cycle, the Aurora-A kinase plays an important role in centrosome maturation and progression to mitosis. In this study, we show in colorectal cell lines that Aurora-A expression is downregulated in response to topoisomerase I inhibition. Using chromatin immunoprecipitation assays, we have observed that the Myc transcription factor and its Max binding partner are associated with the Aurora-A promoter during the G2 phase of the cell cycle. RNA interference experiments indicated that Myc is involved in the regulation of the Aurora-A gene. Following topoisomerase I inhibition, the expression of Myc decreased whereas Mad was upregulated, and the association of Myc and Max with the promoter of the kinase was inhibited. In parallel, an increased association of Mad and Miz-1 was detected on DNA, associated with an inhibition of the recruitment of transcriptional coactivators. Interestingly, a gain of H3K9 trimethylation and HP1 γ recruitment was observed on the Aurora-A promoter following sn38 treatment, suggesting that this promoter is located within SAHF foci following genotoxic treatment. Since Aurora-A is involved in centrosome maturation, we observed as expected that topoisomerase I inhibition prevented centrosome separation but did not affect their duplication. As a consequence, this led to G2 arrest and senescence induction.

These results suggest a model by which the Aurora-A gene is inactivated by the G2 checkpoint following topoisomerase I inhibition. We therefore propose the hypothesis that the coordinated overexpression of Myc and Aurora-A, together with a downregulation of Mad and Miz-1 should be tested as a prognosis signature of poor responses to topoisomerase I inhibitors.

Background

The response to genotoxic treatments relies to a large extent on the activation of the ATM and ATR kinases and on the consequent upregulation of chk1 and chk2 signaling [1-3]. Among numerous substrates, this signaling network leads to the activation and stabilization of the p53 pathway which induces apoptosis or cell cycle arrest [4]. In addition to this protective pathway, others checkpoints are also involved in the control of the progression towards mitosis. At the G1/S transition, chk1/2 activation promotes the degradation of cdc25A by the SCF^{B^TCRP} complex, leading to cdk2 inactivation and G1

phase arrest [5]. During G2 and mitosis, the inhibition of cdc25C by chk1/2 induces the inactivation of cyclin B-cdk1 complexes [6,7], whereas the BubR1, Mad1 or Mad2 proteins can prevent anaphase following spindle checkpoint activation [8].

In association with the cyclin B-cdk1 complexes and cdc25C, the Aurora-A serine/threonine kinase is also essential for progression to mitosis [9,10]. This protein localizes in early G2 to duplicated centrosomes where it plays an important role in their maturation, separation and in the consequent assembly of the spindle apparatus. Illustrating its essential role in spindle organization, the inactivation of Aurora-A leads to the generation of spindle defects, mitotic catastrophe and aneuploidy [10,11]. Importantly, a high expression of the kinase, often due to gene amplification at 20q13, has been

* Correspondence: olivier.coqueret@univ-angers.fr; b.barre@unimedia.fr

† Contributed equally

¹Cancer Center Paul Papin; INSERM U892; Angers, France

Full list of author information is available at the end of the article

detected in several epithelial tumors such as breast, ovarian, gastric, pancreatic and colorectal cancers [9]. In addition, the overexpression of Aurora-A transforms NIH3T3 fibroblasts, probably as a consequence of abnormal mitosis and inactivation of the p53 tumor suppressor gene [12]. An abnormal expression of this kinase is therefore believed to play an important role in cell transformation and genetic instability.

Despite recent studies [13], the regulation of Aurora-A during DNA damage remains most of the time to be characterized. In this study, we show that topoisomerase I inhibitors, one the main drug used in the treatment of colorectal cancers [14,15], induced a downregulation of Aurora-A expression and prevented centrosome separation. In normal conditions, we found that the Myc transcription factor binds to the promoter of this gene in association with Max. Following topoisomerase I inhibition, Myc/Max binding is inhibited, Mad and Miz-1 associate with this promoter and this is associated with transcriptional downregulation.

Altogether, these results indicate that Aurora-A is downregulated in response to topoisomerase I inhibition. We propose that this inhibition plays an important role during the G2 checkpoint in parallel to p53 induction and cdc25C inactivation.

Methods

Reagents

Polyclonal anti-phospho p53 (SC-11764-R), anti-c-myc (SC-764), anti-p21waf1 (SC-397), monoclonal anti-p53 (SC-98), anti-max (C17) (SC-197), anti-mad1 (C19) (SC-222), anti-CBP (A22) (SC369), anti-RNA polymerase II (N20) (SC899), anti-HP1 (S-19) and anti-miz1 (H190) (SC-22837) were obtained from Santa Cruz Biotechnology (Santa Cruz). Monoclonal anti- α and γ -tubulin were obtained from Sigma, anti-H3K9me3 (07-442) and anti-H3-Ac (06-599) were from Upstate. All statistical analysis have been performed with the Graphpad software.

Primers

Total RNA was isolated from cell lines with TRIzol reagent (Invitrogen) and expression was measured by real time PCR analysis using GADPH or RPLPO as a normalization standards. The following primers were used:

Aurora A: For 5'-GATCAGCTGGAGAGCTTAAA-3', Rev 5'-GAGGCTTCCCAACTAAAAAT-3'; c-Myc: For 5'-ATTCTCTGCTCTCCTCGAC-3', Rev 5'-GTAGTTG TGCTGATGTGTGG-3'; Max: For 5'-ACGAAAACG TGGGACCACATC-3', Rev 5'-GTGTGTGGTTTTT CCCGCATAT-3'; Mad: For 5'-GGTTCGGATGAA-CATCCAG-3', Rev 5'-GGCATCTCTGTCCTTGTTA TTGT-3'; Miz-1: For 5'-GGCAAACCTGTCAG AAAA-GAGTAGC-3', Rev 5'-CGCTGCTGGTTCAGC TGTT-

3'; p21WAF1: For 5'-GCTCCTTCCCATCGCTGTCA-3' Rev 5'-TCACCCTGCCCAACCTTAGA-3'; GAPDH: For 5'-GAAGGTGAAGGTCGGAGTC-3', Rev 5'-GAA-GATGGTGTATGGGATTTTC-3'; 3' RPLPO: For 5'-AACC CAGCTCTGGAGAAACT-3' and Rev 5'-CCCCTGGA-GATTTTAGTGGT-3'

Cell lines and treatment

The human colorectal cell lines HT29 (HTB-38) and HCT116 (CCL-247) (ATCC, Manassas, VA20108, USA) were cultured in RPMI 1640 medium (Lonza Walkersville, USA). Cell lines were supplemented with 10% fetal bovine serum (PAA laboratories GmbH, Austria). Cells grown in 3% FBS medium were immediately treated with sn38 (5 ng/ml, 12.5 nM) for 48 h. Note that this treatment should be done before complete cell adhesion so that every cell can incorporate the drug before entering the next S phase. To choose this concentration, clonogenic assays were performed to determine the concentration that kill all cells after 10 days. For HCT116 cells, 5 ng/ml induced 100% mortality.

Chromatin Immunoprecipitation Assay (ChIP)

Cells, grown to 60% confluence, were treated or not as indicated and then washed and cross-linked with 1% formaldehyde at room temperature for 8 min essentially as previously described [16,17]. Reaction was stopped with 10 ml of 125 mM glycine solution. Cells were washed with cold PBS and lysed in 500 μ l of lysis buffer (1% SDS, 10 mM EDTA, 50 mM Tris-HCl pH 8.1, 1 mM PMSF, 5 mM NaF, 5 mM Na3VO4, 2 μ g/ml leupeptin, 5 μ g/ml aprotinin, 1 μ g/ml pestatin), and sonicated five times for 20 secondes each. Supernatants were then recovered by centrifugation at 12 000 rpm for 10 min at 4°C, diluted once in dilution buffer (1% Triton X-100, 2 mM EDTA, 150 mM NaCl, 20 mM Tris-HCl pH 8.1) and subjected to one round of immunoclearing for 2 h at 4°C with 2 μ g of sheared salmon-sperm DNA, and 20 μ l of proteinG-agarose coated with salmon sperm DNA (Millipore) (of 50% slurry). Immunoprecipitation was performed overnight with specific antibodies and IgG control, and then 2 μ g of sheared salmon-sperm DNA and 20 μ l of proteinG-agarose coated with salmon sperm DNA (Millipore) (of 50% slurry) were further added for 1 h at 4°C. Note that immunoprecipitations were performed in the presence of 0,1% Igepal CA-630. Immunoprecipitates were washed sequentially for 10 min each in TSE I (0.1% SDS, 1% Triton X-100, 2 mM EDTA, 20 mM Tris-HCl pH 8.1, 150 mM NaCl), TSE II (0.1% SDS, 1% Triton X-100, 2 mM EDTA, 20 mM Tris-HCl pH 8.1, 500 mM NaCl), and Buffer 3 (250 mM LiCl, 1% NP-40, 1% deoxycholate, 1 mM EDTA, 10 mM Tris-HCl pH 8.1). Beads precipitates were then washed once with TE buffer and eluted once with 1%

SDS, 100 mM NaHCO₃. For Re-ChIP experiments 25 µl of ReChIP buffer (Dilution Buffer, 10 mM DTT) was added to beads following washes and incubated at 37°C for 30 minutes. The sample was then diluted 40 times in dilution buffer and immunoprecipitations, washes and elution were performed as before ([18]). Eluates were heated at 65°C for 6 hours to reverse the formaldehyde cross-linking. DNA was precipitated using classical procedures. Real-time PCR was used for ChIP analysis and quantification. The ChIP have been calculated as binding to region of interest/IgG control, divided by binding to negative control region/IgG control. The following primers were used:

region -668/-400 of the Aurora A promoter: For 5'-GAT GCCCCCTCACTATATGC-3', Rev 5'-AGGAGA GAGCGGGATACCAA-3'; region -114/+161 of the Aurora A promoter: For 5'-AGGCTCTGGCTGGCCGTTG-3', Rev 5'-CCTCGTCCGCCACTGAGATAT-3' Control region -1701/-1399 of the Aurora A promoter For 5'-ACTCCAGATCCCTCAGCTTAACCA-3' Rev 5'-CAAG TTATGGGACGGTGAACG-3'

Other assays

Transient transfections, siRNA knockdown, RNA extraction, semi-quantitative and quantitative reverse transcription-polymerase chain reaction, protein extracts and western blots were all performed as described previously [17,19]. All experiments were performed a minimum of three times before calculating means and standard deviations as shown in figures.

Results

Topoisomerase I inhibition induced a downregulation of Aurora-A expression

We first wanted to confirm in colorectal cell lines that Aurora-A was mainly expressed during the G₂ phase of the cell cycle. To this end, HCT116 cells were synchronized in G₁/S with hydroxyurea, washed and then grown again in serum for 5 to 13 hr. Under these conditions, FACS analysis showed that cells were synchronized after 8-9 hr in the G₂ phase of the cell cycle and that they enter the next G₁ phase after 12-13 hr of serum release (Figure 1A). As expected, we observed that Aurora-A was expressed in G₂, both at the protein (Figure 1B, lanes 1-7) and mRNA levels (Figure 1B, lanes 8-9). The same results were obtained in a second colorectal cell line, the HT29 cells and with different kinds of synchronization such as double thymidine block and serum starvation (data not shown).

To determine whether topoisomerase I inhibition has any influence on Aurora-A expression, HCT116 cells were treated with sn38, the active metabolite of irinotecan [15]. Under these conditions, control cells were synchronized in the G₂ phase of the cell cycle after 48-72

hr (Figure 1C, note that serum 9hr means G₁/S synchronization followed by serum stimulation for 9 hr). Although this was the cell cycle stage when Aurora-A expression was supposed to be maximal, results indicated that the expression of the kinase was downregulated in response to sn38, both at the protein (Figure 1D, compare lane 1 with lanes 2-4) and mRNA levels (Figure 1E, normal mRNAs expression in G₂ was normalized to 1). As a control, the p21waf1 mRNA increased as expected following genotoxic treatment. Finally, these experiments have also been repeated in a different colorectal cell line and sn38 also downregulated Aurora-A in HT29 cells (data not shown and see below Figure 2B).

Altogether, these results indicate that topoisomerase I inhibitors such as sn38 induced a downregulation of Aurora-A expression.

Myc binds to the promoter of the Aurora gene and is involved in its regulation

Following sn38 treatment, we observed as expected in HCT116 cells that p53 was stabilized and phosphorylated on its serine 15 residue. Consequently, p21waf1 level was also enhanced in response to drug treatment (Figure 2A, lanes 1-4). To check whether Aurora-A downregulation was dependent on the p53-p21 pathway [20,21], we used the HCT116 p21^{-/-} derivative cell line in which both p21waf1 alleles have been deleted by homologous recombination [22]. Results showed that sn38 reduced Aurora-A expression in HCT116 p21^{-/-} cells (Figure 2B, lanes 1-4). The same effect was observed in the HT29 cell line that contains a mutated form of p53 (Figure 2B, lanes 5-6). These results indicate that Aurora-A downregulation is not cell-type specific and is independent of the p53-p21 pathway.

During the course of this study, we noticed that the expression of the c-Myc transcription factor was significantly reduced following topoisomerase I inhibition (Figure 2C, lanes 1-4). This suggested that c-Myc was involved in the regulation of the Aurora-A gene. To verify this hypothesis, we used doxycyclin-inducible expression vectors that stably drives the expression of two different Myc siRNAs in two different clones of the LS174T colorectal cell line. As previously shown [17], western blot analysis showed that doxycyclin induced a significant downregulation of c-Myc levels in the two clones (Figure 2D, lanes 4 and 6, top panel). Interestingly, we observed under these conditions that Aurora-A expression was inhibited upon c-Myc knockdown (Figure 2D, compare lanes 4 and 6 with lanes 3 and 5, middle panel). Note that c-Myc downregulation did not modify cell cycle distribution in the G₂ phase of the cell cycle (data not shown) so that Aurora-A inhibition can not be explained by G₀/G₁ arrest.

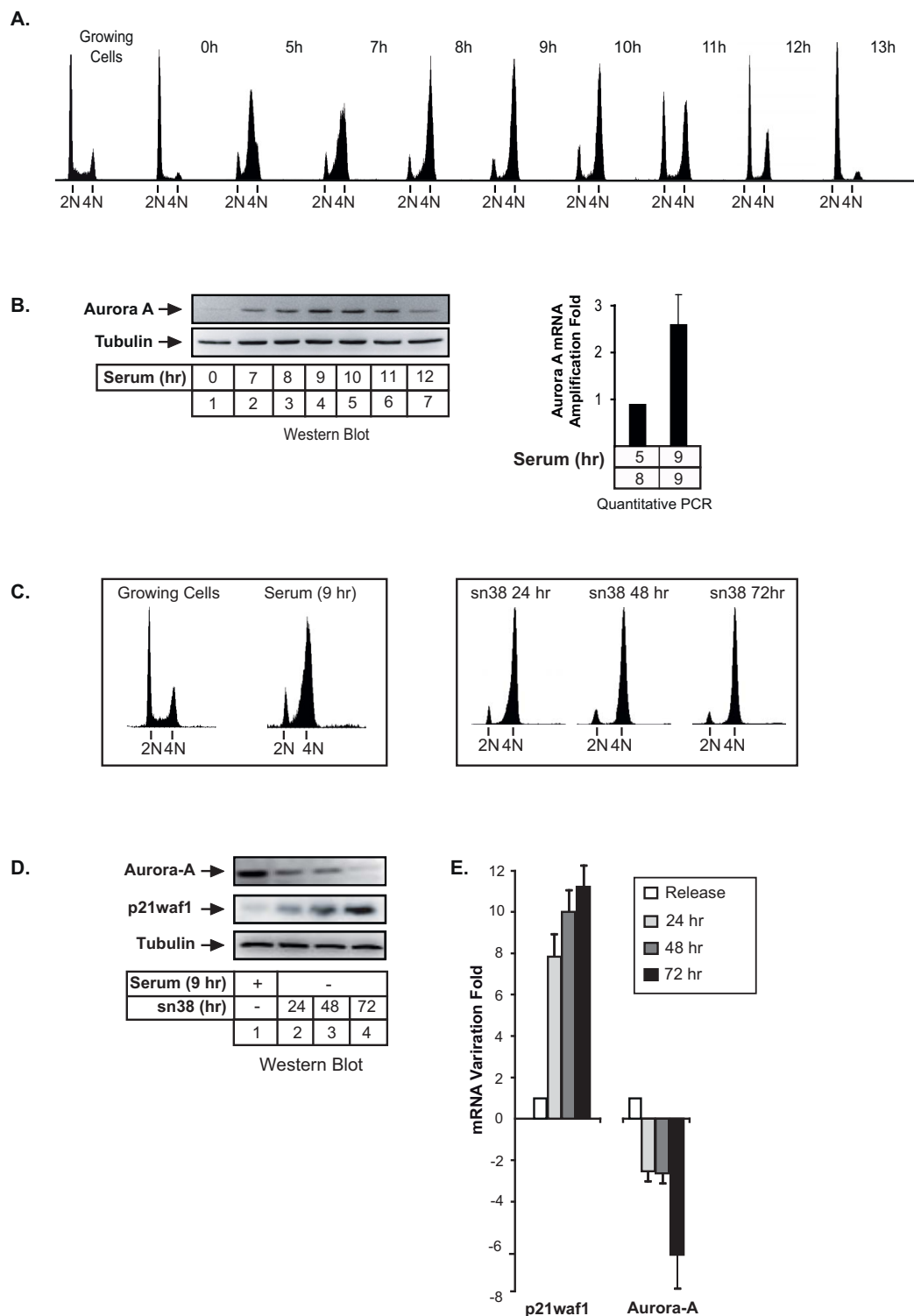


Figure 1 Topoisomerase I inhibition induced a downregulation of Aurora-A expression. A. HCT116 were synchronized in G1/S with hydroxyurea and released for the indicated times in growth medium complemented with 3% serum. DNA content was analyzed by flow cytometry analysis. B. Aurora-A expression was analyzed in these conditions by western blot (lanes 1-7), or quantitative RT-PCR (B, lanes 8-9) ($n = 3 \pm$ sd). C. HCT116 cells were synchronized in the G2 phase of the cell cycle following treatment with hydroxyurea and serum stimulation for 9hr in growth medium (serum 9 hr) or treated with sn38 (5 ng/ml, 12.5 nM). DNA content was then analyzed by flow cytometry and propidium iodide staining. D-E. Aurora-A expression was measured by western blot analysis (D, lanes 1-4) or quantitative RT-PCR (E) following treatment or cell synchronisation. p21waf1 and tubulin expressions were used as controls ($n = 3$).

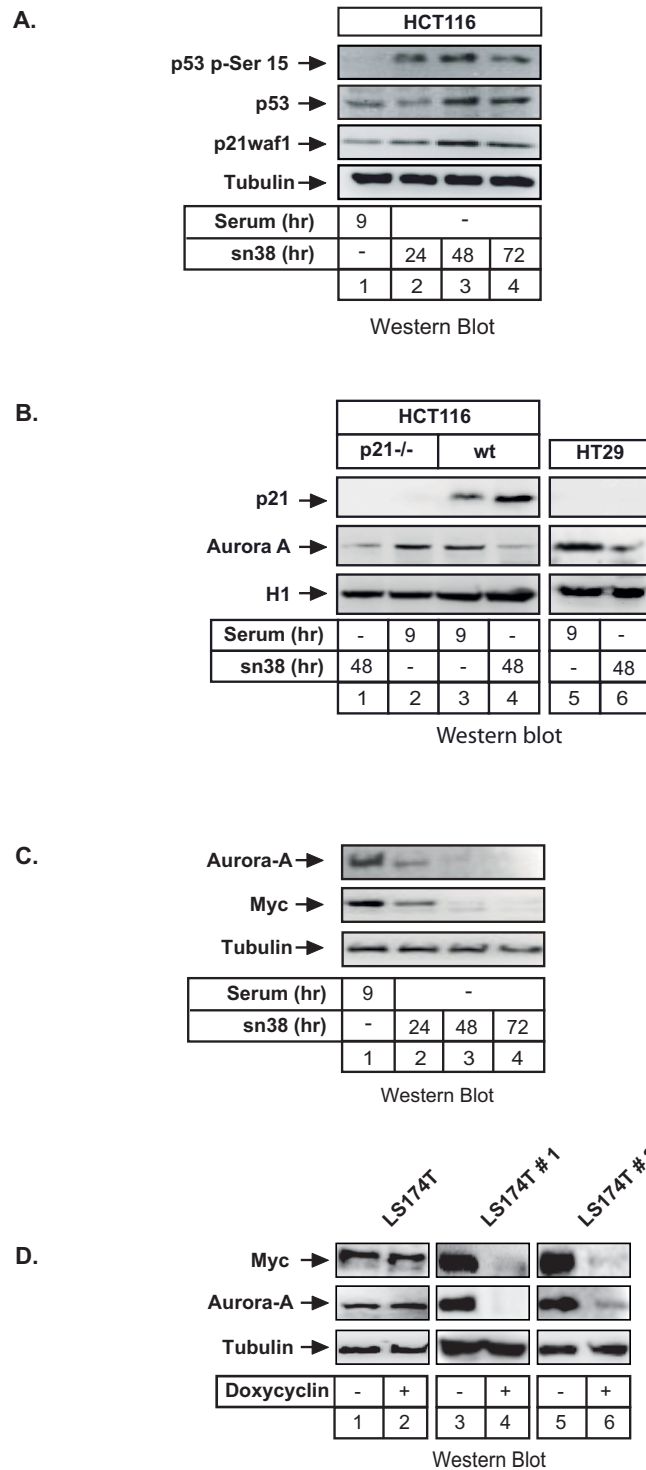


Figure 2 Myc regulates the Aurora-A promoter. A. HCT116 cells were synchronized as above, total cell extracts were prepared and analyzed using antibodies directed against p21waf1, p53 or its serine 15 phosphorylated form (n = 3). B. HCT116 p21^{-/-} or HT29 cells (presenting a mutated form of p53) were treated as described above and Aurora-A and p21waf1 expressions were measured by western blot using tubulin as a control (n = 3). C. HCT116 cells were synchronized in the G2 phase of the cell cycle (serum 9hr) or treated with sn38 for the indicated times. The expression of Myc and Aurora-A was analyzed by western blot on total cell extracts (n = 3). D. LS174T cells were grown in the absence or presence of doxycyclin as indicated. Myc and Aurora expressions were then analyzed by western blot analysis (n = 3). Two different clones of the LS174T colorectal cell line (named LS174T#1 and LS174T#2) were used, each expressing a doxycyclin-inducible expression vector that drives the expression of different siRNAs.

Using the UCSC genome browser <http://genome.ucsc.edu>, we noticed that ChIP-ChIP experiments have already suggested that Myc can potentially bind to the Aurora-A promoter in HeLa cells. Moreover, Ouyang and collaborators have shown by ChIP-seq that both c-Myc and N-Myc can be found associated with this gene in embryonic stem cells [23]. Effectively, transcription factor recognition site analysis of the Aurora-A promoter revealed the presence of non canonical E-boxes that could represent potential Myc binding sites (Figure 3A). To determine if Myc binds to the Aurora A promoter, its recruitment was analyzed by chromatin immunoprecipitation experiments (ChIP) in the LS174T cell line described above. Results presented Figure 3B, lanes 1-4, showed that Myc was effectively recruited to the -668/-400 region of the Aurora-A promoter and that this was associated with histone 3 acetylation (K9), which is indicative of gene transcription. Following siRNA induction and Myc downregulation, the binding of the transcription factor was downregulated and this inhibition was associated with histone H3 deacetylation (Figure 3B, lanes 2 and 4). As a control, no binding of a control IgG (Figure 3B, lanes 5-6), and Myc did not bind to the 5' part of the Aurora-A promoter (data not shown).

Myc is a basic helix-loop-helix zipper transcription factor that heterodimerizes with Max to activate gene transcription. Its activity is inhibited by Mad which associates with Max to recruit repressor complexes to promoters [24]. To determine if Myc and Max are associated with the Aurora-A promoter and if this association is cell cycle dependent, HCT116 cells were synchronized in G1/S with hydroxyurea, washed and then grown again in serum for 5 hr (S/early G2), 9 hr (G2) and 13 hr (next G1). ChIP experiments were then performed as described above. Results presented Figure 3C, lanes 3 and 7, indicate that the two proteins are effectively recruited to this promoter in the G2 phase of the cell cycle. To determine if the two proteins are associated on DNA, a serial ChIP experiment (Re-ChIP) was then performed. For this, the soluble chromatin was immunoprecipitated with Myc antibodies, the immune complexes were released with DTT and the chromatin was further divided into two aliquots and reimmunoprecipitated with IgG or Max antibodies. Under these conditions, subsequent Re-IPs with Max antibodies were able to immunoprecipitate the Aurora-A promoter whereas this was not the case with the control antibody (Figure 3D). Importantly, the association of the two proteins was only detected during the G2 phase of the cell cycle. ChIP result have been obtained by semi-quantitative PCR (Figure 3D, lanes 1-4) and quantified by quantitative-PCR (Figure 3E). As a control, the PCR analysis did not detect any occupancy of a control DNA region (Figure 3D, lanes 5-8) or of the proximal promoter

during the G1 phase of the cell cycle and at the G1/S transition (Figure 3D, lane 4 and 1).

We concluded from these results that the Myc/Max complex binds to the promoter of the Aurora A gene during the G2 phase of the cell cycle and that Myc is involved in the regulation of this gene.

Topoisomerase I inhibition prevents the association of the Myc-Max complex with the Aurora-A promoter

To determine the links between the Myc/Max/Mad pathway and the regulation of the Aurora-A gene following topoisomerase I inhibition, Max/Mad expression was first evaluated following sn38 treatment. Whereas no significant effect was observed on Max expression, Mad levels increased at the protein and mRNA levels (Figure 4A, lanes 1-2 and Figure 4B). As a control, Myc and Aurora-A expressions were downregulated as expected. To determine if the binding of these proteins to the Aurora-A gene was affected by sn38, their recruitment was analyzed by ChIP following treatment. Results showed that the recruitment of Myc and Max was inhibited following topoisomerase I inhibition (Figure 4C, compare lanes 2 and 5, 7 and 9). Note that a weak association of Myc and Max was detected in growing conditions, probably due to the percentage of cells, which are in the G2 phase of the cell cycle (Figure 4C, lanes 1 and 6). Interestingly, these proteins were also found associated with the initiation site, suggesting that the upstream and initiation regions might associate in a transcriptional loop (data not shown). Myc and Max bindings were also inhibited on this initiation site following sn38 treatment. To extend these observations, ChIP experiments were then performed to analyze the recruitment of the Mad protein. In growing conditions or during the G2 phase of the cell cycle, Mad was not found associated with the Aurora-A promoter. Interestingly, when cells were treated with sn38, this protein was significantly recruited to this gene (Figure 4D, lanes 3-4).

Altogether, we concluded from these results that the Myc/Max complex binds to the promoter of the Aurora-A gene in the G2 phase of the cell cycle and that this binding is inhibited upon topoisomerase I inhibition.

Topoisomerase I inhibition promotes Miz-1 recruitment to the Aurora-A promoter

The Miz-1 transcription factor is a POZ-domain-containing zinc-finger protein that can form a transcriptional repressor complex with Myc to inhibit gene transcription [24]. In addition, it has also been proposed that Miz-1 functions as a transcriptional repressor in a Myc-independent manner through its association with cofactors such as BCL6 or Gfi-1 [25,26]. To determine if

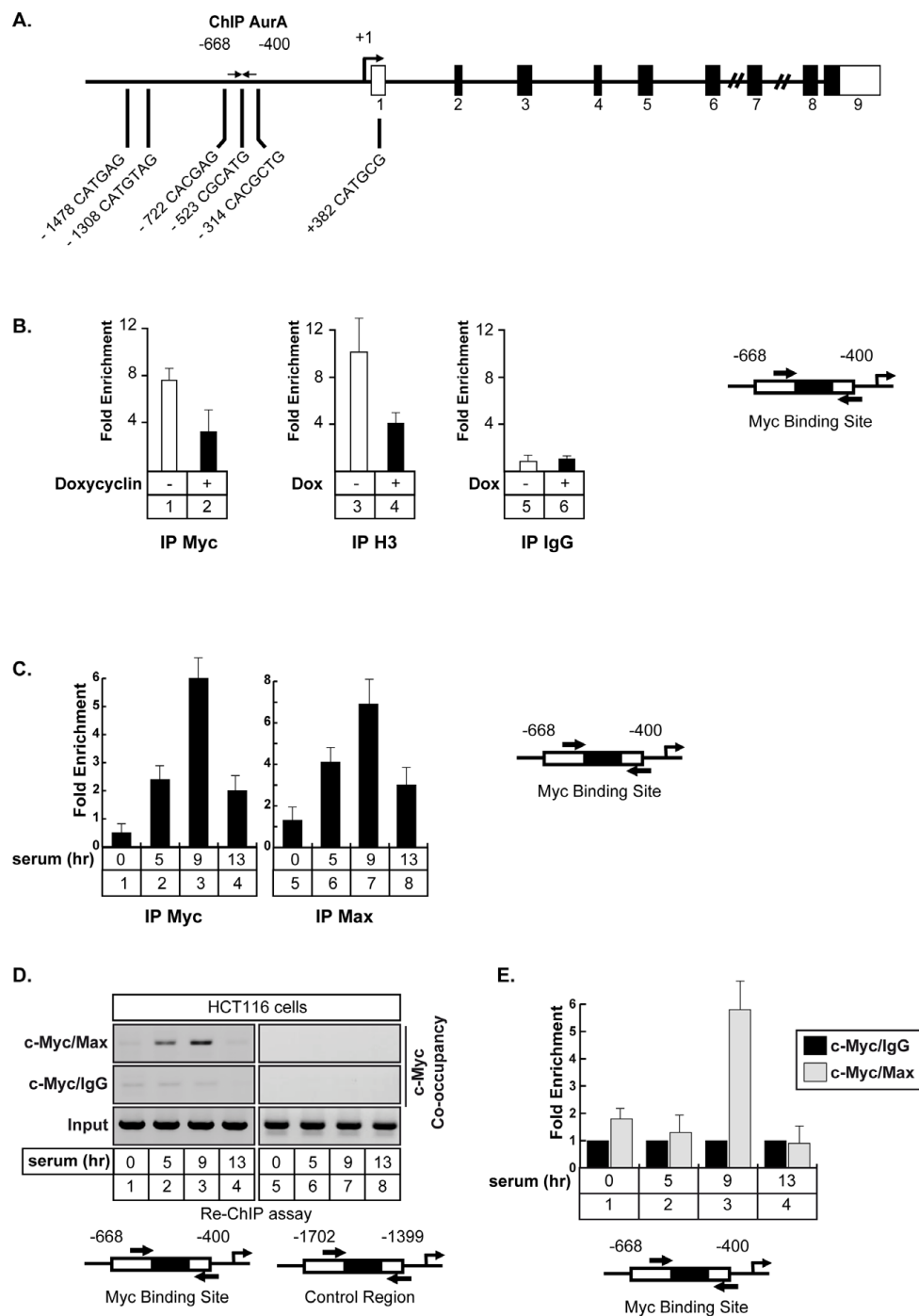


Figure 3 Myc and Max are associated with the Aurora-A promoter. A. Schematic representation of the potential Myc binding sites of the Aurora-A promoter. B. LS174T cells were treated or not with doxycyclin, soluble chromatin was immunoprecipitated with anti-Myc or anti-acetylated-H3 polyclonal antibodies and DNA samples were then amplified using primers that cover the -668/-400 region of the Aurora-A promoter. IgG immunoprecipitations were used as controls (n = 3 +/- sd). C. HCT116 were synchronized in G1/S with hydroxyurea and released for the indicated times in growth medium complemented with 3% serum. Soluble chromatin was immunoprecipitated with anti-Myc or anti-Max antibodies and DNA samples were then amplified using primers that cover the -668/-400 region of the Aurora-A promoter and quantified as compared to IgG immunoprecipitations (n = 3 +/- sd). D, E. The association of Myc and Max on the Aurora-A promoter was analyzed by a serial ChIP experiment. HCT116 were synchronized as described above, the soluble chromatin was immunoprecipitated with Myc antibodies, immune complexes were released and reimunoprecipitated with IgG or Max antibodies. DNA samples were then amplified using primers that cover the -668/-400 region of the Aurora-A promoter and analyzed by semi-quantitative PCR (D) or quantitative PCR (E, n = 3 +/- sd).

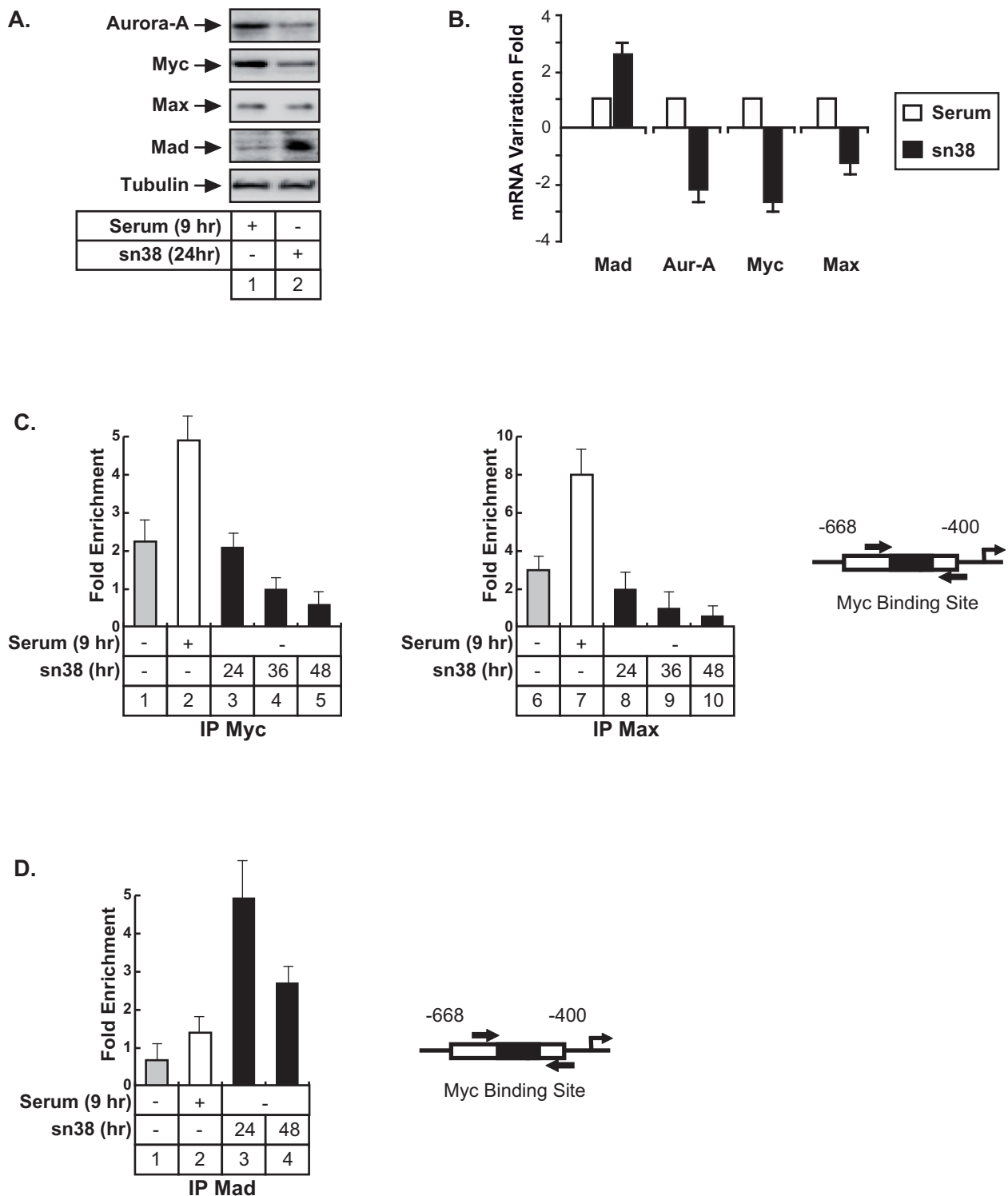


Figure 4 Topoisomerase I inhibition prevents the association of Myc and Max with the Aurora-A promoter. A. HCT116 were synchronized as described above and analyzed by western blot using antibodies directed against the indicated proteins (n = 3). B. Cells were treated as described above and the mRNAs expressions of Aurora-A, Myc, Max and Mad were evaluated by quantitative RT-PCR (n = 3 +/- sd). C-D. The association of Myc, Max and Mad with the Aurora-A promoter was analyzed in HCT116 by chromatin immunoprecipitation as described above (n = 3 +/- sd). ChIPs were performed using extracts isolated from growing cells (C, lanes 1 and 5, D lane 1), from cells synchronized in the G2 phase of the cell cycle (C, lanes 2 and 7, D lanes 2) or from cells treated by sn38 as indicated.

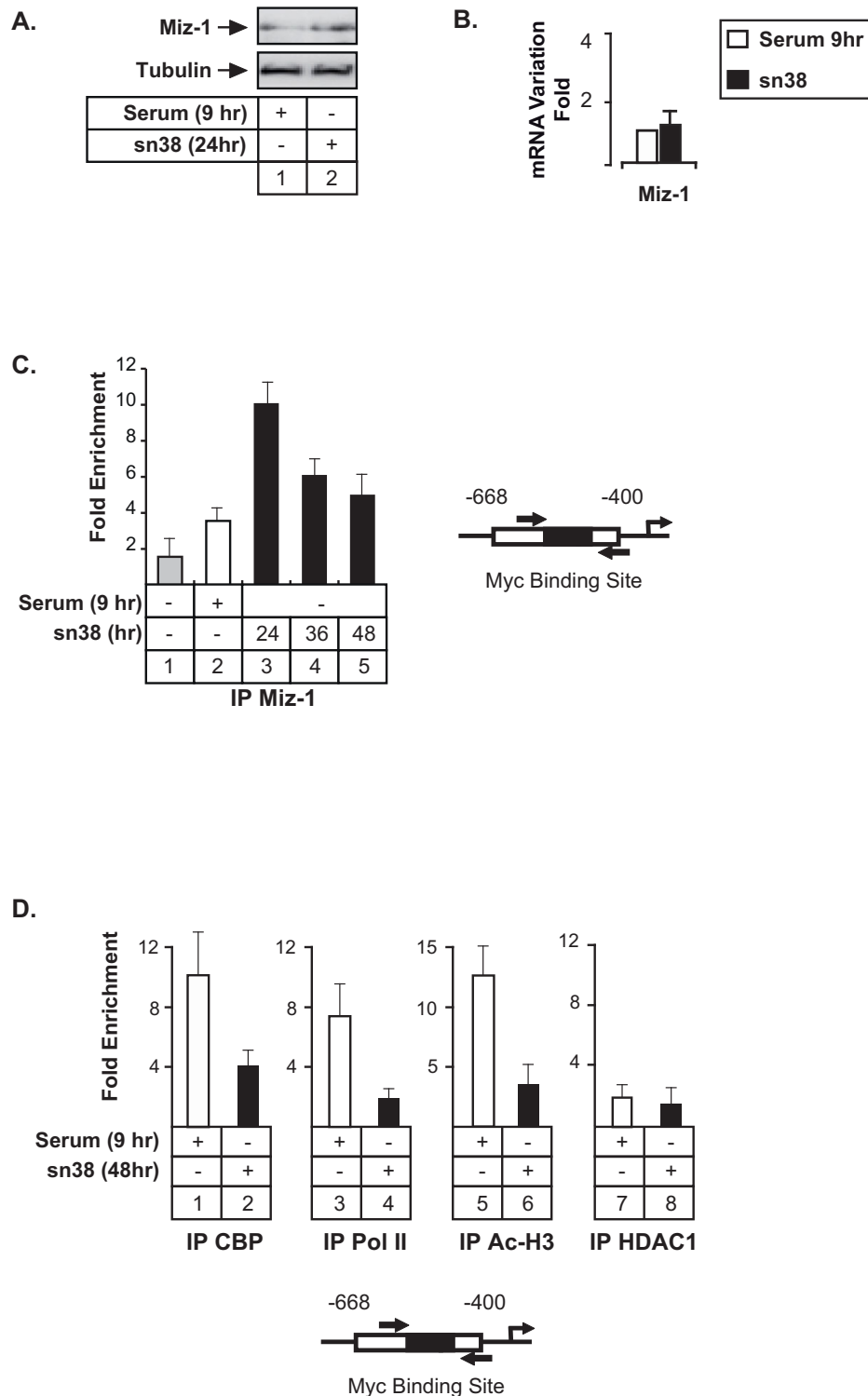


Figure 5 Topoisomerase I inhibition induces the association of Miz-1 with the Aurora-A promoter and prevents the binding of transcriptional coactivators. A-B. HCT116 were treated as described above and Miz-1 expression was analyzed by western blot (n = 3) or quantitative RT-PCR (B, n = 3 +/- sd). C. ChIP analysis of Miz-1 binding to the Aurora-A promoter in growing cells (lane 1), cells synchronized in G2 (lane 2) or following sn38 treatment. D. The recruitment on the Aurora-A promoter of CBP, RNA Pol II, HDAC1 and the acetylation of histone H3 were analyzed by ChIP using soluble chromatin prepared from cells synchronized in the G2 phase of the cell cycle (serum 9hr, lanes 1, 3, 5 and 7) or treated with sn38 (lanes 2, 4, 6 and 8, n = 3 +/- sd).

this protein was involved in Aurora-A inhibition, its expression was evaluated in HCT116 cells treated or not with sn38 (Figure 5A and 5B). Under these conditions, a weak increase in Miz-1 protein level was observed whereas no significant effect was detected on its mRNA expression. ChIP experiments performed in the G2 phase of the cell cycle showed that Miz-1 was associated with the -668/-400 region (Figure 5C, lane 2). By contrast, this protein was not significantly recruited to this gene in growing cells. Interestingly, Miz-1 recruitment was significantly increased following sn38 treatment (Figure 5C, lanes 3-5 and data not shown). Importantly, this binding was associated with a decreased recruitment of the CBP transcriptional coactivator, of the RNA type II polymerase and with a downregulation of histone H3 acetylation (Figure 5D, lanes 2, 4 and 6). We did not observe any recruitment of the HDAC1 histone deacetylase to this promoter.

Altogether, we concluded from these results that topoisomerase I inhibition induces a recruitment of Miz-1 to the Aurora-A promoter and decreases the binding of transcriptional coactivators.

The Aurora-A promoter is located within SAHF foci following topoisomerase I inhibition

We have recently shown that sn38 treatment induced senescence in colorectal cell lines (see [19,27] and text below). Senescence is an irreversible proliferation-arrest that is characterized by the formation of isolated heterochromatin foci called Senescence Associated Heterochromatin Foci (SAHF, [28]). SAHF foci contain marks of transcriptional silencing such as heterochromatin protein 1 (HP1) and tri-methylation of the lysine 9 of histone H3 (H3K9Me3). During senescence, proliferative genes such as E2F targets are compacted within these heterochromatin foci to prevent cell cycle progression, generally as a consequence of Rb-mediated silencing. To extend our results, we then determined if the Aurora-A promoter was included within these SAHFs foci. As a first approach, we used immunofluorescence and western blot experiments to show that sn38 induced a global increase in H3K9 trimethylation in HCT116 cells. As expected, a significant phosphorylation of histone H2Ax was also detected, reflecting the induction of DNA double strand breaks following topoisomerase I inhibition (Figure 6A and 6B). Results were quantified by FACS analysis to show a significant increase of the two signals (Figure 6C). DAPI staining also showed an increase in the presence of punctuate heterochromatin foci in the nucleus of sn38-treated cells which were not detected in control conditions (Figure 6D). ChIP experiments were then used to determine if proteins involved in transcriptional silencing could be found associated with the proximal promoter of the Aurora-A gene

following treatment. Interestingly, results presented Figure 6E, lanes 4-9, showed that HP1 γ was recruited to this gene in sn38-treated cells. In addition, we also noticed a significant increase in the amount of trimethylated H3K9 on the proximal Aurora-A promoter. By contrast, when ChIP experiments were repeated with an antibody directed against the phosphorylated form of histone H2AX, no signs of DNA double strand breaks were detected within this gene.

In light of these results, we concluded that the Aurora-A proximal promoter is located within SAHF foci following genotoxic treatment and that its inhibition is probably related to the recruitment of cofactors involved in transcriptional silencing such as HP1 γ and to the trimethylation of H3K9.

Topoisomerase I inhibition prevents centrosome separation

It has been shown that Aurora-A is involved in the maturation and separation of centrosome during progression from S phase towards mitosis [29]. To determine if topoisomerase I inhibition prevents this maturation, centrosome formation was analyzed by immunofluorescence and γ -tubulin staining. When cells were synchronized in the G2/M phase of the cell cycle, the centrosomes were effectively stained as a doublet and Aurora-A was essentially localized on the centrosomes. As expected, when cells were treated with sn38, Aurora-A became undetectable by immunofluorescence (data not shown). Interestingly, genotoxic treatment did not prevent centrosome duplication, however, no separation was observed under these conditions (Figure 7A). Probably as a consequence of the absence of centrosomal separation and of progression towards mitosis, we observed using clonogenic assays that sn38 induced a complete inhibition of cell proliferation (Figure 7B). Using beta-galactosidase staining, we also noticed an induction of senescence following genotoxic treatment (Figure 7C).

Thus, we concluded from these results that topoisomerase I inhibition prevents centrosome separation, probably as a consequence of Aurora-A inhibition, and that this leads to G2 arrest and senescence induction.

Discussion

In this study, we have shown that the Aurora-A gene is inhibited upon topoisomerase I inhibition. In normal conditions, the Myc transcription factor is recruited to the promoter of the Aurora-A gene in association with its binding partner Max. Following topoisomerase I inhibition, Mad proteins increase, the association of Myc and Max with the Aurora-A promoter is inhibited, the Mad and Miz-1 proteins are recruited to DNA and this is followed by transcriptional downregulation. Probably as a consequence of the downregulation of the Myc-Aurora A

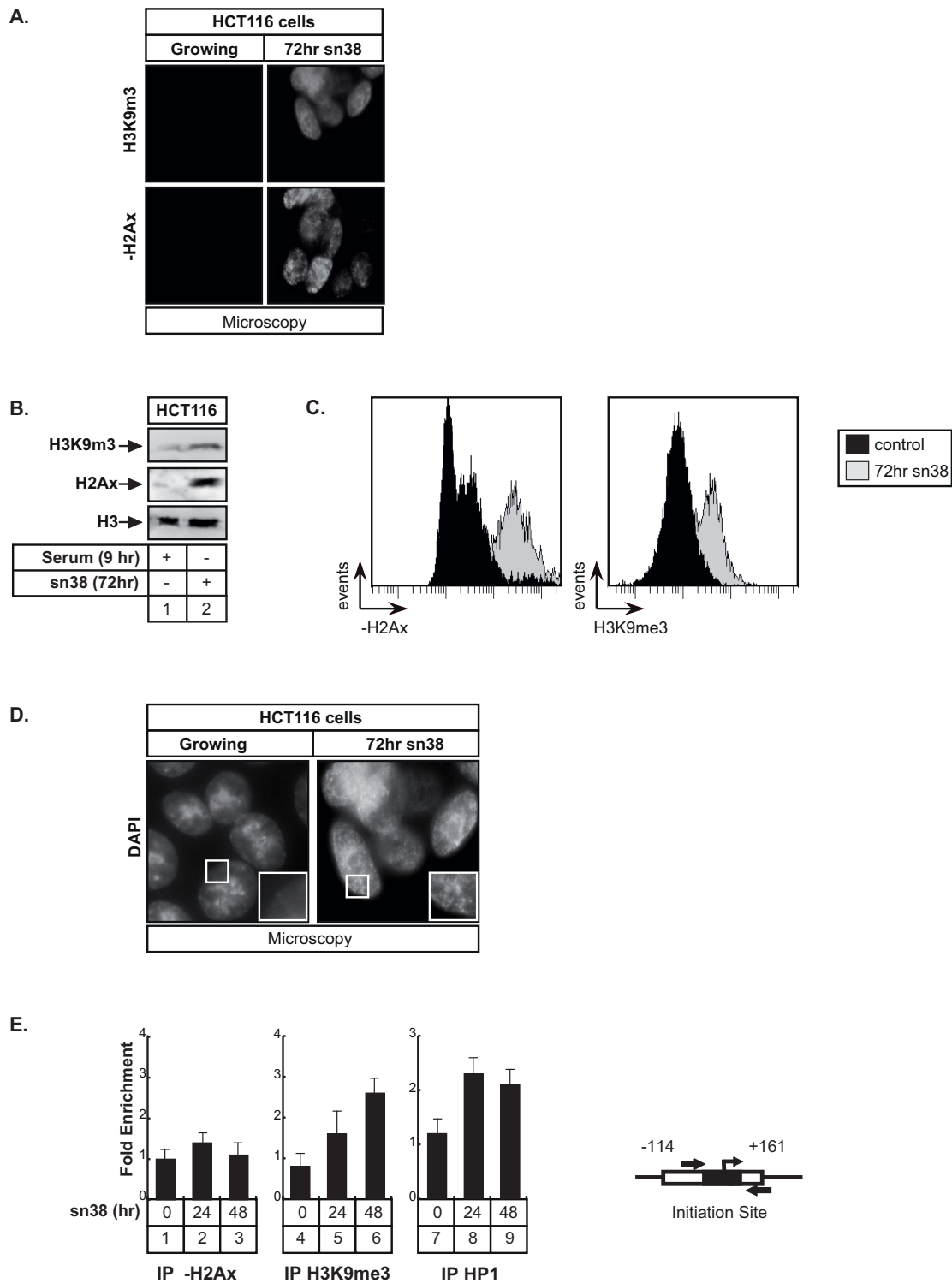
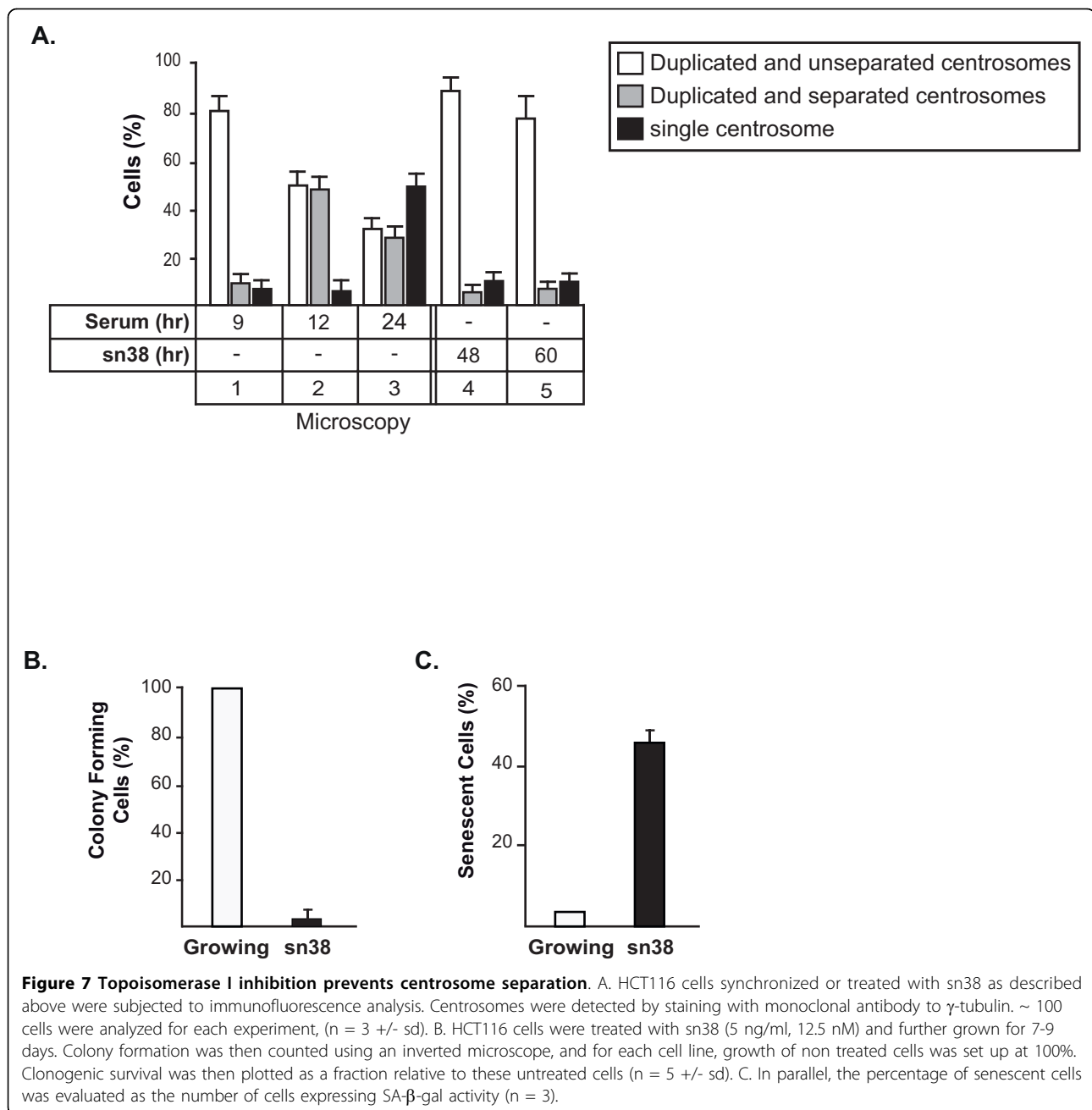


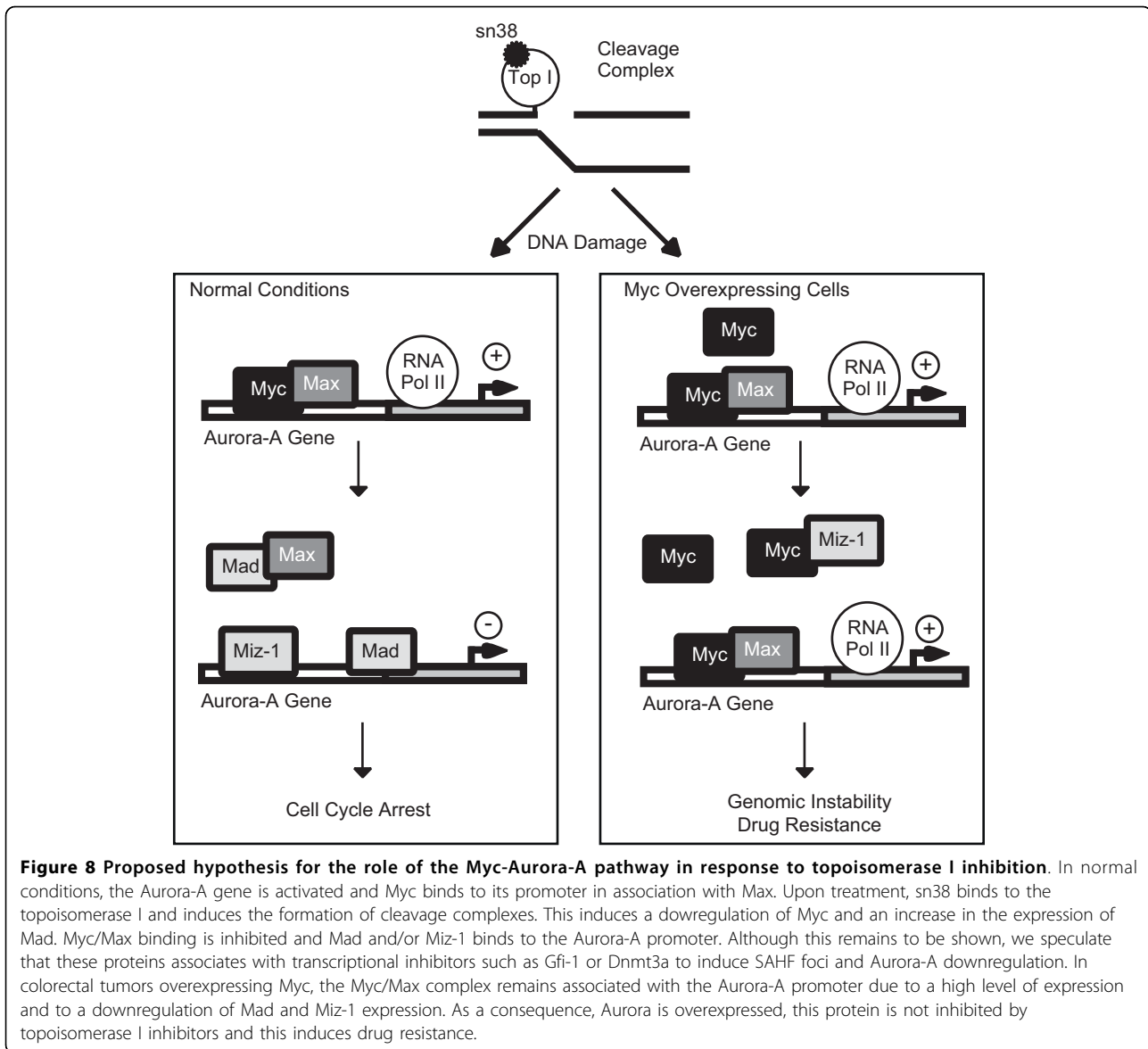
Figure 6 The Aurora-A promoter is located within SAHF foci following sn38 treatment. A, B and C. HCT116 cells were treated with sn38 as described above and H2Ax phosphorylation and H3K9 trimethylation were analyzed by immunofluorescence (A), western blot (B) or FACS (C, n = 3). D. SAHF formation was analyzed in growing cells or following treatment by immunofluorescence using DAPI staining (one experiment representative of three). E. HCT116 were treated as described above and the recruitment on the Aurora-A promoter of HP1 γ , the trimethylation of histone H3K9 and the phosphorylation of histone H2Ax were analyzed by ChIP using soluble chromatin prepared from cells treated or with sn38 (n = 3 +/- sd)



pathway, genotoxic treatment also prevented centrosome separation. In light of these results, we propose that the downregulation of the Aurora-A gene is one of the essential events of G2 arrest occurring in response to topoisomerase I inhibition.

Gene transcription is regulated at multiple steps including DNA binding of transcription factors, recruitment of the basal transcriptional apparatus and elongation of mRNA synthesis. Activation is also affected by several complexes that affect nucleosomal structure [30] such as histone acetyltransferase (HATs) proteins and

chromatin remodeling complexes. In light of our results, we speculate that Myc is associated with Max on the Aurora-A promoter to allow the recruitment of transcriptional coactivators previously shown to be associated with Myc, such as TRAPP, a subunit of the TIP60 histone acetylase complex, or TIP48 and TIP49, two ATPases involved in chromatin remodeling [31]. In addition, Myc can also regulate the elongation program through its association with the P-TEFb complex and cdk9 [32,33]. It will be interesting to determine if Myc regulates the elongation process on the Aurora-A gene as previously



reported on the cad promoter [32,33], or if its effects rely on the recruitment of histone acetylases and chromatin remodeling complexes. We have previously shown that topoisomerase I inhibition induced senescence in colorectal cancers [19]. It has been proposed that this program is associated with chromatin reorganization of proliferation genes into senescence-associated heterochromatin foci (SAHF) [28]. Silencing depends on the retinoblastoma pathway and is associated with enhanced histone H3 tri-methylation and recruitment of the HP1 protein on proliferative genes. Interestingly, we have effectively observed that SAHF are present in colorectal cancer cells treated with sn38 and that topoisomerase I inhibition is associated with the recruitment of HP1 γ and trimethylation of H3K9me3 on the Aurora-A promoter.

Since Miz-1 interacts with transcriptional repressors such as Gfi-1, Dnmt3a or BCL6 to downregulate gene transcription [25,26,34,35], a Miz repressor complex could inactivate the Aurora-A promoter by initiating SAHF formation on this gene. Since SAHF formation has been initially described to be associated with transcriptional silencing induced by the Rb protein, our results also suggest that this gene might be a target of this suppressor pathway. Note however that we have not been able to detect the expression of the p16INK4 protein in our conditions. Thus, if the Aurora-A promoter is regulated by the Rb protein following sn38 treatment, this does probably not rely on p16INK4.

Accumulating evidences indicate that Myc or Aurora A overexpression is associated with chromosomal

instability [10,12,36]. Since both oncogenes play an important role in colorectal cancers, we have started to determine if this oncogenic pathway is associated with genomic instability in colorectal cancers. Preliminary data indicate that the vast majority of colorectal tumors showed a high degree of aneuploidy correlated with an enhanced expression level of Myc and Aurora A. A downregulation of Miz-1 and of the p21waf1 cell cycle inhibitor was also observed. In light of these results, we propose the hypothesis that the dysregulation the Myc-Aurora A pathway is an important event leading to genomic instability through the bypass of the G2/M checkpoints. We speculate that tumors expressing abnormal levels of Myc together with a high expression of Aurora-A might be resistant to DNA-topoisomerase I inhibitors such as irinotecan. The downregulation of the p21waf1 protein is also probably an essential event to allow the inactivation of the senescence program. For this reason, we propose the hypothesis that the coordinated overexpression of Myc and Aurora-A, together with a downregulation of Miz-1 should be tested as a prognosis signature of poor responses to topoisomerase I inhibitors (Figure 8). This signature should help to define in advance the subsets of tumors that will fail to respond to chemotherapy.

Conclusions

Following DNA damage, the ATM/ATR/chk pathway is activated to induce the upregulation of the p53 tumor suppressor and the consequent activation of the p21waf1 gene. In parallel, the cdc25 phosphatases are inactivated, leading to cdk inhibition and cell cycle arrest. Using colorectal cancer cell lines, we show that the Aurora-A gene is also downregulated following topoisomerase I inhibition and that this effect is probably related to a decreased recruitment of the Myc transcription factor to its promoter. We propose the hypothesis that tumors expressing high levels of the Myc-Aurora-A pathway might be resistant to topoisomerase I inhibitors.

Acknowledgements

This work was supported by a fellowship (to A.V. and S.C.) and a grant from Institut National du Cancer and from the Ligue contre le Cancer (Equipes labélisées 2007 to O.C., C.P. and E.G.), a grant from Canceropole Grand Ouest (O.C., C.P. and E.G.) and a fellowship from INSERM-Region and Rotary (to J.C.).

Author details

¹Cancer Center Paul Papin; INSERM U892; Angers, France. ²Cancer Center Paul Papin; Biopathology Department, France. ³CNRS UMR 6061, Université de Rennes I, IFR140, France. ⁴EA 3142, Université d'Angers, France.

Authors' contributions

JC, SC performed most experiments, including mRNA, protein, ChIPs and cell cycle analysis and SC also helped editing the manuscript. AV made senescence and proliferation assays whereas MBT did cloning experiments.

SG and IV analyzed the data. EG, CP, BB and OC provided the suggests and wrote the paper. All authors read and approved the final manuscript.

Competing interests

The authors declare that they have no competing interests.

Received: 16 March 2010 Accepted: 3 August 2010

Published: 3 August 2010

References

1. Bartek J, Lukas J: Chk1 and Chk2 kinases in checkpoint control and cancer. *Cancer Cell* 2003, **3**:421-429.
2. Su TT: Cellular responses to DNA damage: one signal, multiple choices. *Annu Rev Genet* 2006, **40**:187-208.
3. Rajagopalan H, Lengauer C: Aneuploidy and cancer. *Nature* 2004, **432**:338-341.
4. Vousden KH, Lu X: Live or let die: the cell's response to p53. *Nat Rev Cancer* 2002, **2**:594-604.
5. Mailand N, Falck J, Lukas C, Syljuasen RG, Welcker M, Bartek J, Lukas J: Rapid destruction of human Cdc25A in response to DNA damage. *Science* 2000, **288**:1425-1429.
6. Peng CY, Graves PR, Thoma RS, Wu Z, Shaw AS, Piwnicka-Worms H: Mitotic and G2 checkpoint control: regulation of 14-3-3 protein binding by phosphorylation of Cdc25C on serine-216. *Science* 1997, **277**:1501-1505.
7. Sanchez Y, Wong C, Thoma RS, Richman R, Wu Z, Piwnicka-Worms H, Elledge SJ: Conservation of the Chk1 checkpoint pathway in mammals: linkage of DNA damage to Cdk regulation through Cdc25. *Science* 1997, **277**:1497-1501.
8. Fang G, Yu H, Kirschner MW: The checkpoint protein MAD2 and the mitotic regulator CDC20 form a ternary complex with the anaphase-promoting complex to control anaphase initiation. *Genes Dev* 1998, **12**:1871-1883.
9. Zhou H, Kuang J, Zhong L, Kuo WL, Gray JW, Sahin A, Brinkley BR, Sen S: Tumour amplified kinase STK15/BTAK induces centrosome amplification, aneuploidy and transformation. *Nat Genet* 1998, **20**:189-193.
10. Giet R, Petretti C, Prigent C: Aurora kinases, aneuploidy and cancer, a coincidence or a real link? *Trends Cell Biol* 2005, **15**:241-250.
11. Meraldi P, Honda R, Nigg EA: Aurora kinases link chromosome segregation and cell division to cancer susceptibility. *Curr Opin Genet Dev* 2004, **14**:29-36.
12. Meraldi P, Honda R, Nigg EA: Aurora-A overexpression reveals tetraploidization as a major route to centrosome amplification in p53^{-/-} cells. *Embo J* 2002, **21**:483-492.
13. Krystyniak A, Garcia-Echeverria C, Prigent C, Ferrari S: Inhibition of Aurora A in response to DNA damage. *Oncogene* 2006, **25**:338-348.
14. Pommier Y, Redon C, Rao VA, Seiler JA, Sordet O, Takemura H, Antony S, Meng L, Liao Z, Kohlhaagen G, et al: Repair of and checkpoint response to topoisomerase I-mediated DNA damage. *Mutat Res* 2003, **532**:173-203.
15. Pommier Y: Topoisomerase I inhibitors: camptothecins and beyond. *Nat Rev Cancer* 2006, **6**:789-802.
16. Bienvenu F, Barre B, Giraud S, Avril S, Coqueret O: Transcriptional Regulation by a DNA-associated Form of Cyclin D1. *Mol Biol Cell* 2005, **16**:1850-1858, Epub 2005 Jan 1819.
17. Barré B, Vigneron A, Coqueret O: The STAT3 transcription factor is a target for the Myc and retinoblastoma proteins on the Cdc25A promoter. *J Biol Chem* 2005, **280**:15673-15681.
18. Barre B, Perkins ND: The Skp2 promoter integrates signaling through the NF-kappaB, p53, and Akt/GSK3beta pathways to regulate autophagy and apoptosis. *Mol Cell* 2010, **38**:524-538.
19. Vigneron A, Gamelin E, Coqueret O: The EGFR-STAT3 oncogenic pathway up-regulates the Eme1 endonuclease to reduce DNA damage after topoisomerase I inhibition. *Cancer Res* 2008, **68**:815-825.
20. Vigneron A, Cherier J, Barre B, Gamelin E, Coqueret O: The cell cycle inhibitor p21waf1 binds to the myc and cdc25A promoters upon DNA damage and induces transcriptional repression. *J Biol Chem* 2006, **281**:34742-34750.
21. Vigneron A, Roninson IB, Gamelin E, Coqueret O: Src inhibits adriamycin-induced senescence and G2 checkpoint arrest by blocking the induction of p21waf1. *Cancer Res* 2005, **65**:8927-8935.

22. Waldman T, Lengauer C, Kinzler KW, Vogelstein B: **Uncoupling of S phase and mitosis induced by anticancer agents in cells lacking p21.** *Nature* 1996, **381**:713-716.
23. Ouyang Z, Zhou Q, Wong WH: **ChIP-Seq of transcription factors predicts absolute and differential gene expression in embryonic stem cells.** *Proc Natl Acad Sci USA* 2009, **106**:21521-21526.
24. Wanzel M, Herold S, Eilers M: **Transcriptional repression by Myc.** *Trends Cell Biol* 2003, **13**:146-150.
25. Phan RT, Saito M, Basso K, Niu H, Dalla-Favera R: **BCL6 interacts with the transcription factor Miz-1 to suppress the cyclin-dependent kinase inhibitor p21 and cell cycle arrest in germinal center B cells.** *Nat Immunol* 2005, **6**:1054-1060.
26. Basu S, Liu Q, Qiu Y, Dong F: **Gfi-1 represses CDKN2B encoding p15INK4B through interaction with Miz-1.** *Proc Natl Acad Sci USA* 2009, **106**:1433-1438.
27. Courapied S, Sellier H, De Carne Trecesson S, Vigneron A, Bernard AC, Gamelin E, Barre B, Coqueret O: **The cdk5 kinase regulates the STAT3 transcription factor to prevent DNA damage Upon topoisomerase I inhibition.** *J Biol Chem* 2010, PMID: 20516069.
28. Narita M, Nunez S, Heard E, Narita M, Lin AW, Hearn SA, Spector DL, Hannon GJ, Lowe SW: **Rb-mediated heterochromatin formation and silencing of E2F target genes during cellular senescence.** *Cell* 2003, **113**:703-716.
29. Kramer A, Lukas J, Bartek J: **Checking out the centrosome.** *Cell Cycle* 2004, **3**:1390-1393.
30. Kingston RE, Narlikar GJ: **ATP-dependent remodeling and acetylation as regulators of chromatin fluidity.** *Genes Dev* 1999, **13**:2339-2352.
31. Adhikary S, Eilers M: **Transcriptional regulation and transformation by Myc proteins.** *Nat Rev Mol Cell Biol* 2005, **6**:635-645.
32. Eberhardy SR, Farnham PJ: **c-Myc mediates activation of the cad promoter via a post-RNA polymerase II recruitment mechanism.** *J Biol Chem* 2001, **276**:48562-48571.
33. Eberhardy SR, Farnham PJ: **Myc recruits P-TEFb to mediate the final step in the transcriptional activation of the cad promoter.** *J Biol Chem* 2002, **277**:40156-40162.
34. Herold S, Wanzel M, Beuger V, Frohme C, Beul D, Hillukkala T, Syvaioja J, Saluz HP, Haenel F, Eilers M: **Negative regulation of the mammalian UV response by Myc through association with Miz-1.** *Mol Cell* 2002, **10**:509-521.
35. Wanzel M, Kleine-Kohlbrecher D, Herold S, Hock A, Berns K, Park J, Hemmings B, Eilers M: **Akt and 14-3-3eta regulate Miz1 to control cell-cycle arrest after DNA damage.** *Nat Cell Biol* 2005, **7**:30-41.
36. Vafa O, Wade M, Kern S, Beeche M, Pandita TK, Hampton GM, Wahl GM: **c-Myc can induce DNA damage, increase reactive oxygen species, and mitigate p53 function: a mechanism for oncogene-induced genetic instability.** *Mol Cell* 2002, **9**:1031-1044.

doi:10.1186/1476-4598-9-205

Cite this article as: Courapied *et al.*: Regulation of the Aurora-A gene following topoisomerase I inhibition: implication of the Myc transcription Factor. *Molecular Cancer* 2010 **9**:205.

Submit your next manuscript to BioMed Central and take full advantage of:

- Convenient online submission
- Thorough peer review
- No space constraints or color figure charges
- Immediate publication on acceptance
- Inclusion in PubMed, CAS, Scopus and Google Scholar
- Research which is freely available for redistribution

Submit your manuscript at
www.biomedcentral.com/submit



The cdk5 Kinase Regulates the STAT3 Transcription Factor to Prevent DNA Damage upon Topoisomerase I Inhibition*

Received for publication, December 7, 2009, and in revised form, May 10, 2010. Published, JBC Papers in Press, June 1, 2010, DOI 10.1074/jbc.M109.092304

Sandy Courapied¹, H el ene Sellier¹, Sophie de Carn e Tr ecesson, Arnaud Vigneron, Anne-Charlotte Bernard, Erick Gamelin, Benjamin Barr e, and Olivier Coqueret²

From the Paul Papin Cancer Center, INSERM U892, 2 rue Moll, 49933 Angers, France

The STAT3 transcription factors are cytoplasmic proteins that induce gene activation in response to growth factor stimulation. Following tyrosine phosphorylation, STAT3 proteins dimerize, translocate to the nucleus, and activate specific target genes involved in cell-cycle progression. Despite its importance in cancer cells, the molecular mechanisms by which this protein is regulated in response to DNA damage remain to be characterized. In this study, we show that STAT3 is activated in response to topoisomerase I inhibition. Following treatment, STAT3 is phosphorylated on its C-terminal serine 727 residue but not on its tyrosine 705 site. We also show that topoisomerase I inhibition induced the up-regulation of the cdk5 kinase, a protein initially described in neuronal stress responses. In co-immunoprecipitations, cdk5 was found to associate with STAT3, and pulldown experiments indicated that it associates with the C-terminal activation domain of STAT3 upon DNA damage. Importantly, the cdk5-STAT3 pathway reduced DNA damage in response to topoisomerase I inhibition through the up-regulation of Eme1, an endonuclease involved in DNA repair. ChIP experiments indicated that STAT3 can be found associated with the Eme1 promoter when phosphorylated only on its serine 727 residue and not on tyrosine 705. We therefore propose that the cdk5-STAT3 oncogenic pathway plays an important role in the expression of DNA repair genes and that these proteins could be used as predictive markers of tumors that will fail to respond to chemotherapy.

Signal transducer and activator of transcription 3 (STAT3)³ proteins are cytoplasmic transcription factors that translocate into the nucleus following growth factor stimulation. In contrast to normal cells where its phosphorylation is only transient, constitutive activation of STAT3 has been reported in several primary cancers and tumor cell lines (1–3). This abnormal activation is due to oncogenic kinases such as epidermal growth

factor receptor, Her2/Neu, src, or bcr-abl, which induce STAT3 activation through phosphorylation of its tyrosine 705 residue (4). This phosphorylation allows the nuclear translocation and DNA binding of the STAT3 dimer and the up-regulation of several genes involved in cell-cycle and cell survival such as *cyclin D1*, *Myc*, or *bclxl*. The up-regulation of these cancer genes mediates the oncogenic activity of STAT3 and its ability to transform cells (5).

A second phosphorylation occurs on the serine 727 residue of the C-terminal activation domain. It has been proposed that this phosphorylation is necessary for maximal gene activation, because its mutation prevents STAT3 transcriptional function (6). It is believed that this modification favors the recruitment of transcriptional cofactors such as CBP, NcoA, or P-Tefb that binds to the C-terminal domain of the transcription factor (7–10). However, it remains to be determined if the association of STAT3 with its coactivators is a direct consequence of Ser-727 phosphorylation.

Although it was initially believed that the tyrosine phosphorylation is essential for STAT3 activity, several groups have recently reported that specific forms of the transcription factor, which are only phosphorylated on its Ser-727 residue, can induce gene activation. In prostate cancer, Ser-727 phosphorylation is sufficient to activate STAT3 and drive tumorigenesis in the absence of tyrosine 705 activation (11). Elegant results have shown that tyrosine 705 mutants can associate with NF- κ B and induce the expression of genes such as *mras* or *met*, which are likely to play an important role in cell transformation by STAT3 (12–14). These results lead to the important conclusion that the influence of STAT3 on cell transformation can be independent of the tyrosine 705 phosphorylation and that this site should not be considered as a unique marker of STAT3 oncogenic activity.

This conclusion also leads to the hypothesis that STAT3 can induce different transcriptional programs, depending on which sites are phosphorylated and certainly on the type of stimulation. Although STAT3 activation is well characterized in response to growth factor stimulation, little is known about its regulation in response to other stimulation such as DNA damage and chemotherapy treatment. Interestingly, several studies have suggested that an abnormal activation of this transcription factor is associated with intrinsic drug resistance (15). STAT3 expression has been associated with resistance to radiation-induced apoptosis (16–18), and it can also confer resistance to Fas or paclitaxel-mediated apoptosis in multiple myeloma and ovarian cancer (19, 20). Most of the time, escape to drug treatment is related to the STAT3-mediated expression of survival

* This work was supported by fellowships (to S. C. and A. V.), by a grant (Equipe Labelis ee) from the Ligue Contre le Cancer and Institut du Cancer, and a fellowship from Inserm-Pays de Loire (to S. C. T.), and by the Minist ere de la Recherche (to H. S.).

¹ Both authors contributed equally to this work.

² To whom correspondence should be addressed: Centre R egional de Lutte Contre le Cancer Paul Papin, INSERM U892 2 rue Moll, 49033 Angers, France. Tel.: 33-2-41-35-29-14; E-mail: olivier.coqueret@univ-angers.fr.

³ The abbreviations used are: STAT3, signal transducers and activators of transcription 3; ChIP, chromatin immunoprecipitation; CBP, CREB-binding protein; cdk, cyclin-dependent kinase; siRNA, small interference RNA; PBS, phosphate-buffered saline; RT, reverse transcription; IL-6, interleukin-6; FACS, fluorescent-activated cell sorting.

The *cdk5-STAT3-Eme1* Pathway Prevents DNA Damage

proteins such as bcl-xl or survivin (21, 22). In addition, we have recently shown that the epidermal growth factor receptor-src-STAT3 pathway can prevent senescence induction (23) and activate DNA repair genes (24) to confer resistance to chemotherapy treatments.

In this study, we have further characterized the regulation of STAT3 during DNA damage. In colorectal cell lines, we have found that the transcription factor is phosphorylated on its serine 727 residue following topoisomerase I inhibition and that tyrosine 705 phosphorylation is not modified. In addition, we have also observed that this phosphorylation is due to the binding of the *cdk5* kinase to the transcription factor. *cdk5* is a serine/threonine kinase, which was initially characterized in postmitotic neurons. Once associated with its specific activators p35/p25, this protein plays an important role in neuronal survival, neurite outgrowth, and cytoskeletal functions (25–27). In response to topoisomerase I inhibition, we have observed that *cdk5* is activated and that it interacts with STAT3 to induce its serine phosphorylation. *Cdk5* appeared to be involved in the STAT3-mediated regulation of the *cyclin D1*, *myc*, and *Eme1* genes. Importantly, ChIP analysis showed that the transcription factor can be found associated with the *Eme1* promoter when phosphorylated only on serine 727. We therefore propose that *cdk5* regulates the STAT3-*Eme1* pathway and that this is an important step in the response of colorectal tumors to topoisomerase I inhibition.

MATERIALS AND METHODS

Cell Lines—The human colorectal cell lines HT29 (HTB-38) and HCT116 (CCL-247) (ATCC, Manassas, VA) were cultured in RPMI 1640 medium (Lonza, Walkersville, MD). Cell lines were supplemented with 10% fetal bovine serum (PAA Laboratories GmbH, Austria).

Materials—sn38 came from Pfizer (New York, NY). Polyclonal anti-STAT3 (C20), anti-phospho-STAT3-Ser-727 (ser727-R), anti-*cdk5* (C8), anti-*cdk5* Y15, anti-Erk2 (C14), anti-phospho-Erk1/2 (E4), anti-p35 (C19), anti-lamin A/C (346), anti- β -tubulin (H-235), and hsc70 (B-6) were obtained from Santa Cruz Biotechnology (Santa Cruz, CA). The anti-H2Ax Alexa fluor was obtained from BD Biosciences, and the anti-phospho-STAT3-Tyr 705 was from Cell Signaling. The *cdk5* and STAT3 siRNAs have been obtained from Dharmacon Inc. (Lafayette, CO) and transfected using the Dharmafect 4 (Dharmacon) method. Three different siRNAs were used for each transfection.

Cell Treatment—Cells grown in 3% FBS medium were immediately treated with sn38 (5 ng/ml) for 48 h. Note that this treatment should be done before complete cell adhesion so that every cell can incorporate the drug before entering the next S phase. For siRNA experiment, cells were transfected with the appropriate siRNA using the Dharmafect 4 method and grown up for 48 h in 6-well plates. In 3% FBS medium, cells were then divided into two wells and again immediately treated with sn38 (5 ng/ml) for 48 h.

Immunoprecipitation and Western Blot Analysis—After two washings with cold PBS, cells were lysed in 100 μ l (Western blot) or 1 ml (immunoprecipitation) using ice-cold lysis buffer (25 mM HEPES, pH 7.9, 300 mM KCl, 0.2 mM EDTA, 10% gly-

cerol, 1 mM phenylmethylsulfonyl fluoride, 2 μ g/ml leupeptin, 5 μ g/ml aprotinin, 1 μ g/ml pepstatin A, 0.5 M NaF, 100 mM Na_3VO_4). After a 30-min incubation at 4 $^\circ\text{C}$, total extracts were clarified by centrifugation at 12,000 rpm for 10 min.

Immunoprecipitations were performed overnight at 4 $^\circ\text{C}$ with whole cell extracts (2–4 mg) in the presence of 0.1 or 1% Nonidet P-40 (CA-630, Sigma). Cell extracts were precleared with 75 μ l of protein G-agarose (Sigma-Aldrich, 50% slurry in phosphate-buffered saline) for 2 h at 4 $^\circ\text{C}$, and cleared extracts were immunoprecipitated with 4 μ g of the indicated antibodies overnight at 4 $^\circ\text{C}$ followed by the addition of 50 μ l of protein G-agarose for 1 h at 4 $^\circ\text{C}$. Immunoprecipitated proteins were washed two times in lysis buffer and one time with 10 mM Tris, pH 8, 100 mM EDTA, prior to the addition of sample buffer. Following electrotransfer, membranes (Millipore Corp., Billerica, MA) were blocked for 45 min at room temperature in Tris-buffered saline buffer, 5% bovine serum albumin, 0.05% Tween. Membranes were then incubated overnight with the indicated antibodies diluted in Tris-buffered saline buffer, 1% bovine serum albumin, 0.05% Tween at 4 $^\circ\text{C}$. After three washings, blots were incubated with the appropriate horseradish peroxidase-conjugated secondary antibody for 45 min. Proteins were detected using an enhanced chemiluminescence system (ECL, Bio-Rad).

Quantitative PCR—RNA was extracted using the TRIzol method (Invitrogen), and complementary DNA was synthesized from 2 μ g of RNA by random hexamer priming using Moloney murine leukemia virus reverse transcriptase (Promega, Madison, WI). For cDNA quantification, PCR was performed with 4 μ l of 20 \times diluted cDNA, 5 μ l of Qiamix (Qiagen), and 1 μ l of 5 μM primers. Accumulation of fluorescent products was monitored on the ABI PRISM 7300 real-time PCR system (Applied Biosystems, Foster City, CA). The relative quantification of gene expression was performed using the comparative C_T method, with normalization of the target gene to the endogenous housekeeping gene RPLPO. RT-PCR primers were as follows: RPLPO (5'-AACCCAGC-TCTGGAGAAACT-3' and 5'-CCCCTGGAGATTTAGTGGT-3'), CD1 (5'-CAGTAACGTCACACGGACTAC-3' and 5'-ACAGGAGCTGGTGTTCAT-3'), *cdk5* (5'-AGCGACA-AGAAGCTGACTTT-3' and 5'-AGAATCCCAGCCCTTT-AGT-3'), and *Eme1* (5'-AACGCTTCAGGCCTTTGTAA-3' and 5'-GCTCCCTGTTCCCTCTTCT-3').

ChIP—Attached cells were washed twice with cold PBS, cross-linked with 1% formaldehyde at room temperature for 10 min, and then washed twice with 10 ml of cold PBS. Cells were lysed with 500 μ l of lysis buffer (1% SDS, 10 mM EDTA, 150 mM NaCl, 20 mM Tris-HCl, pH 8.1, 1 mM phenylmethylsulfonyl fluoride, 2 μ g/ml leupeptin, 5 μ g/ml aprotinin, 1 μ g/ml pepstatin A, 0.5 M NaF, 100 mM Na_3VO_4), and extracts were sonicated six times for 15 s each. Supernatants were recovered by centrifugation at 12,000 rpm for 10 min at 4 $^\circ\text{C}$, diluted one time in dilution buffer (1% Triton X-100, 20 mM Tris-HCl, pH 8.1, 2 mM EDTA, 150 mM NaCl, 1 mM phenylmethylsulfonyl fluoride, 2 μ g/ml leupeptin, 5 μ g/ml aprotinin, 1 μ g/ml pepstatin A, 0.5 M NaF, 100 mM Na_3VO_4), and subjected to one round of immunoclearing for 2 h at 4 $^\circ\text{C}$ using protein-G-agarose coated with salmon sperm DNA (Millipore). Immunoprecipitations were

performed overnight with specific antibodies, then 20 μ l of protein G-agarose-coated beads with salmon sperm DNA (50%) was added for 1 h at 4 °C. Beads were then washed for 10 min in TSE1 (0.1% SDS, 1% Triton X-100, 2 mM EDTA, 20 mM Tris-HCl, pH 8.1, and 150 mmol NaCl), TSE2 (0.1% SDS, 1% Triton X-100, 2 mM EDTA, 20 mM Tris-HCl, pH 8.1, and 500 mmol NaCl), and TSE3 (0.25 M LiCl, 1% Nonidet P-40, 1% deoxycholate, 1 mM EDTA, and 10 mM Tris-HCl, pH 8.1). Beads were washed once with TE buffer (10 mM Tris, pH 8, 100 mM EDTA) and eluted with 500 μ l of elution buffer (1% SDS and 0.1 M NaHCO₃) for 1 h. Eluates were heated at 65 °C overnight, and DNA was precipitated using classic procedures. For PCR, 5 μ l from a 100- μ l DNA preparation was used for 25–30 amplification cycles. The following primers were used: region –34/+89, 5'-CCGGGCTTTGATCTTTGCT-3' and 5'-GACTCTGCTGCTCGCTGCTA-3' of the cyclin D1 promoter; region –2760/–2486, 5'-TTGTGCCACTGCTGACTTTGTC-3' and 5'-AGCCTGAAGAAGGAGGATGTGAGG-3' of the p21 promoter. Myc and Eme1 primers have been described before (24, 28).

Flow Cytometry—For DNA content analysis, 1.5×10^6 cells were washed twice with PBS and fixed in 70% ethanol. Cells were treated with 100 units/ml RNase A for 20 min at 37 °C, then diluted in PBS/propidium iodide (50 μ g/ml), and immediately analyzed by flow cytometry (BD Biosciences). For phospho-H2Ax analysis, 1×10^6 cells were recovered by centrifugation with their supernatant at 1500 rpm for 5 min at room temperature. Cells were fixed with 2% paraformaldehyde at room temperature for 10 min. Cells were then washed twice with PBS and centrifuged at 1500 rpm for 5 min at 4 °C. Cells were incubated with a PBS-2% bovine serum albumin-0.2% Triton solution for 2 min. The primary antibody was diluted at 1/50, and 4',6-diamidino-2-phenylindole (5 μ g/ml) was diluted 500 times. Cells were incubated for 1 h at room temperature and then analyzed by flow cytometry.

Colony Formation Assay—For colony formation assays, 1000 cells were plated per well in 6-well plates, treated with sn38 the next day and allowed to form colonies. After 10–14 days cells were washed twice with PBS and treated with crystal violet for 10 min at room temperature, and then washed five times with water. The percentage of colony-forming cells was calculated as compared with non-treated cells.

Pulldown Assay—Bacteria were grown up in 5 ml of LB medium overnight. 200 ml of ampicillin-LB was inoculated with 2 ml of the overnight culture and grown up until optical density reached 0.6–0.8. Isopropyl 1-thio- β -D-galactopyranoside was then added at 1 mM for 2 h, bacteria were recovered by centrifugation at 4000 rpm for 20 min at 4 °C, resuspended in 8 ml of lysis buffer (50 mM Na₂HPO₄, pH 8, 300 mM NaCl, 10 mM imidazole, 1 mM phenylmethylsulfonyl fluoride, 1 mg/ml lysozyme), incubated on ice for 30 min and sonicated 6–8 times for 20 s. Triton X-100 was added to the final concentration of 1% and incubated on ice for 15 min. Extracts were recovered by centrifugation at 4000 rpm for 15 min at 4 °C, and supernatants were transferred to a 15-ml conical tube. 250 μ l of beads (nickel-nitrilotriacetic acid-agarose, Qiagen) was added for every 200 ml of initial culture, and extracts were incubated for 1 h at 4 °C. Beads were then washed three times with washing buffer (50 mM Na₂HPO₄, pH 8, 300 mM NaCl, 20 mM imidazole, 1 mM

phenylmethylsulfonyl fluoride). Beads (400 ng of fusion protein) were then incubated for 20 min at 4 °C with cell extracts (300 μ g) and washed three times with lysis buffer (25 mM HEPES, pH 7.9, 300 mM KCl, 0.2 mM EDTA, 10% glycerol, 1 mM phenylmethylsulfonyl fluoride, 2 μ g/ml leupeptin, 5 μ g/ml aprotinin, 1 μ g/ml pepstatin A, 0.5 M NaF, 100 mM Na₃VO₄) prior to the addition of sample buffer and Western blot analysis.

Kinase Assay—His- Δ 1–716 STAT3 proteins were produced as described above and eluted from the beads. In parallel, cdk5 was immunoprecipitated from sn38-treated cells (total extracts, 100 μ g), and 15 μ l of beads was incubated with 1 μ g of His- Δ 1–716 STAT3 at room temperature for 10 min with 10 μ M cold ATP. The reaction was stopped by the addition of 50 μ l of sample buffer. Samples were analyzed by Western blot as described above using a polyclonal antibody directed against the serine-phosphorylated form of STAT3.

RESULTS

STAT3 Is Phosphorylated on Its Serine 727 Residue following Topoisomerase I Inhibition—To determine if the STAT3 transcription factor is involved in the response to DNA damage, growing HT29 colorectal cells were treated with sn38, the active metabolite of irinotecan. Using Western blot analysis, we observed that topoisomerase I inhibition induced the phosphorylation of STAT3 on its serine 727 C-terminal residue (Fig. 1A, lanes 3 and 4). As a control, topoisomerase I inhibition did not affect the expression or phosphorylation of the Erk1/2 kinases (Fig. 1B, lanes 1 and 2). Because p53 is mutated in the HT29 cell line, this effect does not appear to rely on the tumor suppressor gene. Under these conditions, we were not able to detect a significant activation of the tyrosine 705 phosphorylation site, whereas this site was normally phosphorylated upon IL-6 stimulation. When HT29 cells were serum-starved for 2 days and then stimulated with this cytokine for 30 min, a significant activation of the two phosphorylation sites was detected as expected (Fig. 1C, lanes 1 and 2). In addition, when the transcription factor was immunoprecipitated using antibodies directed against its tyrosine 705-phosphorylated form, we observed that STAT3 was phosphorylated on its two sites following IL-6 stimulation. However, we were not able to detect any tyrosine phosphorylation following topoisomerase I inhibition (Fig. 1C, compare lanes 4 and 5). Using Western blot analysis, we observed that this phosphorylation remained non-detectable during the 3 days of treatment, whereas the serine 727 phosphorylation was easily detected and declined at 96 h (Fig. 1D, lanes 1–4 and data not shown). Note, however, that we were able to detect a weak constitutive phosphorylation of the tyrosine 705 site when 600 μ g of total extract was used. By contrast, 50–60 μ g of proteins were used in this study to detect all protein expression and STAT3 serine 727 phosphorylation. Therefore, in our experimental model, the tyrosine-phosphorylated forms of STAT3 are not highly expressed as compared with the ones presenting a phosphorylation on the serine 727 residue.

The activation of STAT3 was surprising, because its phosphorylation theoretically occurs in the G₁ phase of the cell cycle and in response to growth factor stimulation. Under the conditions used in this study, clonogenic assays indicated that sn38

The *cdk5*-STAT3-*Eme1* Pathway Prevents DNA Damage

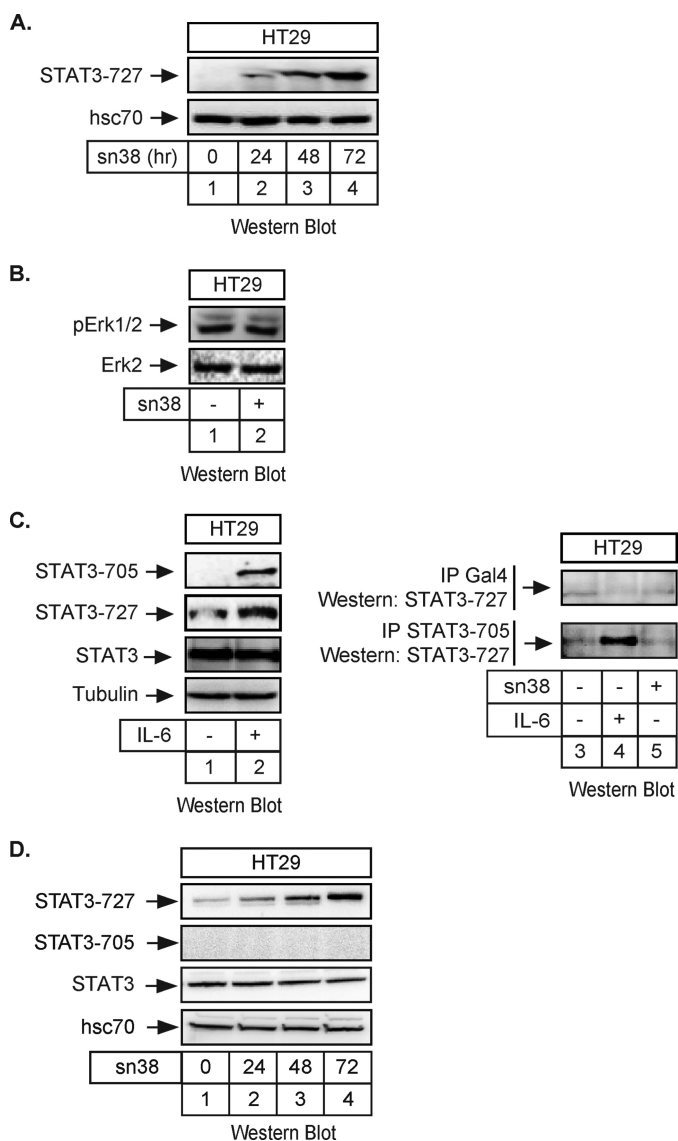


FIGURE 1. STAT3 is phosphorylated on its serine 727 residue following topoisomerase I inhibition. *A*, HT29 cells were treated with sn38 (5 ng/ml) or not for the indicated times. Following stimulation, total cell extracts were prepared, and serine 727 phosphorylation was analyzed by Western blot using polyclonal antibodies directed against the phosphorylated form of the protein. The membrane was reprobed with an antibody directed against hsc70 as a loading control ($n = 5$). Note that, in every experiment, sn38 was added to the cell culture just after cell plating to get an optimal inhibition of cell cycle progression. *B*, HT29 cells were treated with sn38 (5 ng/ml) for 48 h. Following stimulation, cell extracts were prepared and p-Erk1/2 and Erk2 expression was analyzed by Western blot with polyclonal antibodies directed against these proteins ($n = 3$). *C*, HT29 cells were serum-starved for 2 days and stimulated with IL-6 (20 ng/ml) for 30 min. STAT3 activation was analyzed by Western blot using antibodies directed against the different phosphorylated forms of the proteins or against its non-phosphorylated form ($n = 2$). In parallel, whole cell extracts were immunoprecipitated with polyclonal antibodies directed against the tyrosine-phosphorylated form of STAT3 (–705) or control antibodies (Gal4), and samples were then analyzed by Western blot using polyclonal antibodies directed against STAT3 Ser727 ($n = 2$). *D*, HT29 cells were treated with sn38 (5 ng/ml) or not for the indicated times. Following stimulation, total cell extracts were prepared, and the serine 727 and tyrosine 705 phosphorylations were analyzed by Western blot using polyclonal antibodies directed against the phosphorylated forms of the protein. The membrane was reprobed with an antibody directed against STAT3 and then hsc70 as a loading control ($n = 3$).

treatment inhibited cell proliferation, and FACS analysis showed that HT29 cells were arrested in the G_2 phase of the cell cycle after 48 h (Fig. 2A). Because STAT3 phosphorylation is

maximal at 72 h, this event is probably not driving G_2 arrest. To confirm that STAT3 was activated during the G_2 phase of the cell cycle upon DNA damage, FACS experiments were performed using propidium iodide staining conjugated with intracellular staining using phospho-serine 727 antibodies. Cells were treated with sn38 or starved and stimulated with IL-6 as a control. As expected, upon cytokine stimulation, the two main STAT3 phosphorylation sites, serine 727 (and tyrosine 705, data not shown) were detected mainly in cells present in the G_1 phase of the cell cycle. By contrast, serine phosphorylation following sn38 treatment was detected essentially in the G_2 phase of the cell cycle (Fig. 2B).

We noticed that a fraction of HT29 cells died by apoptosis following sn38 treatment as shown by the reproducible presence of a sub G_1 propidium iodide staining (Fig. 2A, right panel). This escape to G_2 arrest has been previously reported and is due to the inactivation of the p53-p21^{waf1} pathway in this cell line (29). To determine if STAT3 phosphorylation was due to the induction of apoptosis, we used HCT116 cells, because topoisomerase I inhibition induces senescence in this cell line due to intact p53 signaling. Results presented in Fig. 2C confirm that sn38 induced G_2 arrest and the appearance of cells with multiple micronuclei and an increase in the number of β -galactosidase-positive cells, two hallmarks of senescence induction and mitotic catastrophe. Under this condition, Western blot analysis showed that STAT3 was phosphorylated on its serine 727 residue to the same extent as compared with HT29 cells (Fig. 2C, lanes 1 and 2). This result suggests that the phosphorylation of the transcription factor is not due to apoptosis. Importantly, it also indicates that this effect is not cell line-specific. Altogether, these results indicate that the STAT3 transcription factor is phosphorylated on its serine 727 residue in response to topoisomerase I inhibition.

The *cdk5* Kinase Is Up-regulated upon Topoisomerase I Inhibition—We then wanted to determine which kinase is involved in STAT3 phosphorylation upon genotoxic treatment. During the course of these experiments, we have noticed that the expression of the *cdk5* kinase was increased in response to topoisomerase I inhibition. Although *cdk5* has been essentially characterized in neurons (25), it has been recently shown that this protein is also involved in the response to DNA damage and in the induction of senescence programs (30–33). Interestingly, this kinase has also been shown to regulate STAT3 in neuronal cells (34). Using total cell extracts, Western blot experiments showed that *cdk5* expression was significantly enhanced in response to sn38 (Fig. 3A, lanes 2 and 3). As a control, we did not detect any significant activation of p38, although it was phosphorylated as expected in response to the rasV12 oncogene (Fig. 3A, lanes 4–6). To determine if the increased expression of the kinase was regulated at the transcriptional level, cells were treated with sn38, and the level of the *cdk5* mRNA was analyzed by quantitative RT-PCR experiments. Results presented Fig. 3B showed that topoisomerase I inhibition had no effect on this mRNA, suggesting that the expression of *cdk5* was mainly regulated at the translational level. In neuronal cells, it has been shown that *cdk5* is activated following its association with its p35/p25 coactivator (25). Western blot experiments showed that p35 was constitutively expressed in HT29 cells and

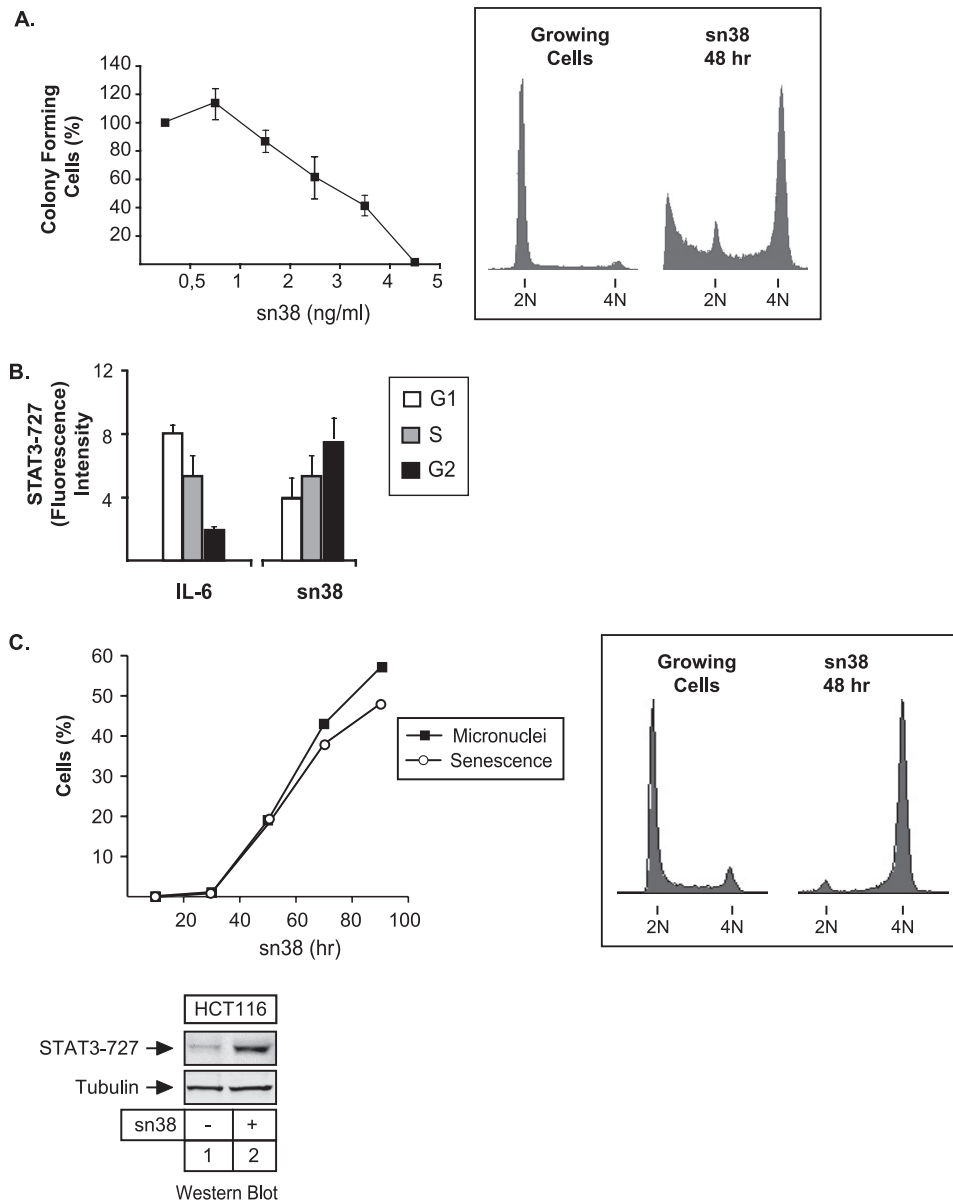


FIGURE 2. STAT3 is phosphorylated on serine 727 during G₂ arrest. A, HT29 cells were treated or not with different concentration of sn38 for 10–14 days. Colony formation was then counted using an inverted microscope, and the growth of non-treated cells was set up at 100%. Clonogenic survival was then plotted as a fraction relative to these untreated cells ($n = 5 \pm$ S.D.). In parallel, growing HT29 cells were treated with sn38 (5 ng/ml) for 48 h, and DNA content and apoptosis were then evaluated by flow cytometry ($n = 5$). B, HT29 cells were treated with sn38 (5 ng/ml) or IL-6 (20 ng/ml) as indicated, and DNA content and serine phosphorylation were then analyzed by flow cytometry analysis using polyclonal antibodies directed against the serine 727-phosphorylated form of STAT3 ($n = 3$). C, growing HCT116 cells were treated or not with sn38 for different times as indicated. The percentage of senescent cells was evaluated as the number of cells expressing SA- β -gal activity and micronuclei (left part, $n = 3$). In parallel, DNA content was evaluated by flow cytometry after 48 h (right part), and the phosphorylation of STAT3 on its serine residue was analyzed by Western blot as described above ($n = 3$, bottom).

that sn38 did not affect its expression level (Fig. 3C, lanes 1 and 2). We were not able to detect p25. We then asked whether *cdk5* interacts with p35 upon drug treatment. To this end, HT29 cells were treated with sn38, total cell extracts were recovered, and co-immunoprecipitations were performed with polyclonal antibodies directed against p35 or nonspecific antibodies (Fig. 3C, lanes 3–6). Proteins present in the immunoprecipitates were revealed by immunoblotting with anti-*cdk5* antibodies. Under these conditions, *cdk5*

was found to co-immunoprecipitate with p35 proteins (Fig. 3C, compare lane 6 and 4). Note that these co-immunoprecipitations were carried out using non-transfected cells, so that the association does not require the proteins to be overexpressed. It has been recently proposed that the binding to p35 is not sufficient to initiate *Cdk5* kinase activation, which is also dependent on the phosphorylation of the kinase on its tyrosine 15 residue (35). We thus determined using total cell extracts whether sn38 also modulates *Cdk5* phosphorylation. As shown in Fig. 3D, lanes 1–4, we found that phosphorylation of *Cdk5* at tyrosine 15 was also increased in response to topoisomerase I inhibition. Note that, using total cell extracts, we were not able to detect a significant activation of the kinase before 48 h of treatment (see below). Therefore, we concluded from these results that the *cdk5* kinase is activated following topoisomerase I inhibition.

Cdk5 Interacts with STAT3 and Induces Its Serine 727 Phosphorylation upon Topoisomerase I Inhibition—To determine if *cdk5* is involved in STAT3 serine phosphorylation following sn38 treatment, we first asked if the kinase could bind to the transcription factor. To this end, HT29 cells were treated with sn38, total cell extracts were recovered, and immunoprecipitations were performed with polyclonal antibodies directed either against STAT3 or nonspecific antibodies (Fig. 4A, lanes 1 and 2). Proteins present in the immunoprecipitates were revealed by immunoblotting with the reciprocal *cdk5* or STAT3 antibodies. Under these conditions, STAT3 was found to co-immunoprecipitate with *cdk5*.

These interactions were specific, because almost no interaction was observed using a control IgG antibody (Fig. 4A, compare lanes 1 and 2). Importantly, these co-immunoprecipitations were performed with extracts from non-transfected cells; therefore, the association between STAT3 and *cdk5* did not rely on the overexpression of the two proteins.

To confirm this observation, *in vitro* pulldown experiments were performed using bacterially produced 6 \times histidine-tagged STAT3 containing either the full-length protein or the

The cdk5-STAT3-Eme1 Pathway Prevents DNA Damage

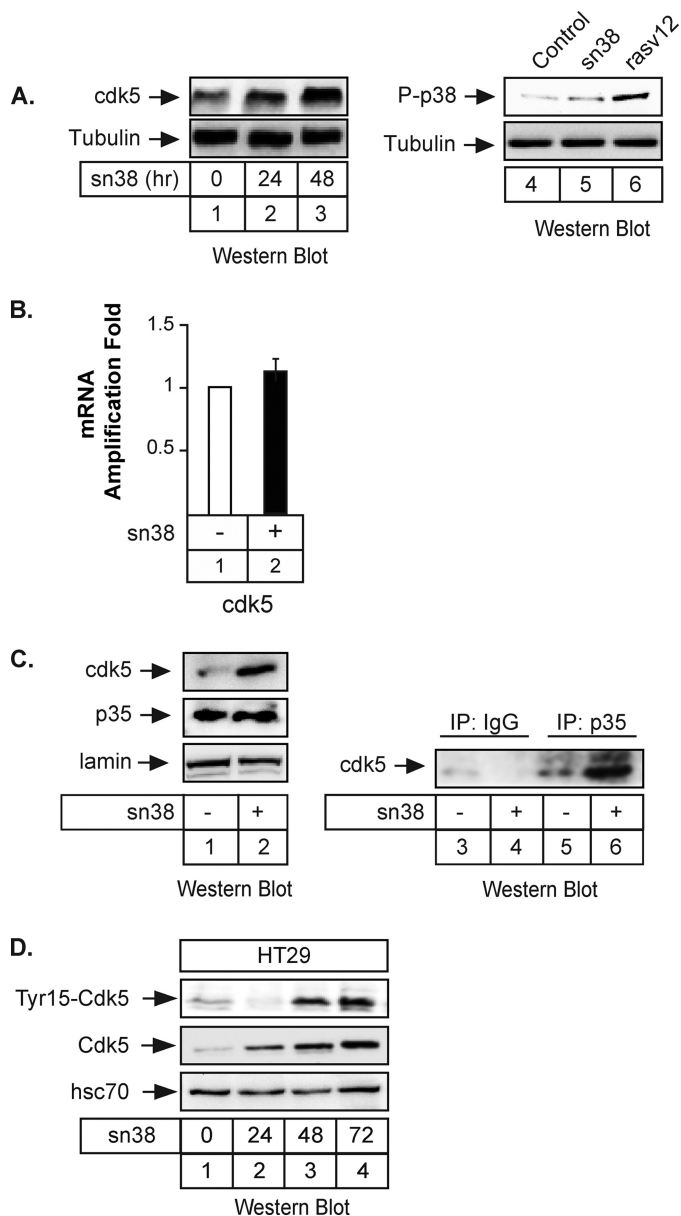


FIGURE 3. The cdk5 kinase is activated following topoisomerase I inhibition. *A*, growing HT29 cells were treated or not with sn38 (5 ng/ml) for 24 or 48 h. Following stimulation, total cell extracts were prepared, and cdk5 expression was analyzed by Western blot using polyclonal antibodies directed against the kinase (lanes 1–3, $n = 5$). Under the same conditions, the phosphorylation of the p38 kinase was investigated. As a control, cells were transfected with the rasv12 oncogene to induce p38 activation (lanes 4–6, $n = 3$). The membranes were reprobbed with an antibody directed against tubulin as a loading control. *B*, growing HT29 cells were incubated with sn38 (5 ng/ml) for 48 h, and the expression of the cdk5 mRNA was analyzed by quantitative RT-PCR experiments ($n = 3$). *C*, growing HT29 cells were treated as described above, and after 48 h, whole cell extracts were prepared and Western blot analysis was performed with polyclonal antibodies directed against cdk5, p35, or lamin as a loading control (lanes 1 and 2). In parallel, extracts were immunoprecipitated with polyclonal antibodies directed against p35 (lanes 5 and 6) or a control serum (lanes 3 and 4). Samples were then analyzed by Western blot using polyclonal antibodies directed against cdk5 ($n = 3$). *D*, HT29 cells were treated with sn38 as described previously, and the expression and phosphorylation of cdk5 on its tyrosine 15 residue were analyzed by Western blot ($n = 3$).

716–770 amino acids corresponding to the activation domain of STAT3 (Fig. 4*B*, STAT3 or STAT3 Δ 1–716). His-tagged STAT3 proteins were immobilized on beads and incubated

with total cell extracts prepared from cells treated or not with sn38. As previously shown using extracts from neuronal cells (34), we found that the endogenous cdk5 kinase was retained by the full-length his-STAT3 protein as well as by the STAT3 Δ 1–716 fusion protein immobilized on beads. By contrast, the kinase was not retained by the beads alone (Fig. 4*C*, compare lanes 3–5). We also noticed that this interaction was dependent on sn38, because almost no signal was observed using extracts from non-treated cells (Fig. 4*C*, compare lanes 1–2 with 3–4).

We then determined if cdk5 was involved in the serine phosphorylation of STAT3 in response to genotoxic treatment. To this end, cells were transfected with a pool of three siRNA directed against cdk5 or the corresponding control siRNA, cells were treated or not, and STAT3 phosphorylation was then investigated by Western blot. Following siRNA transfection, we observed as expected that the expression of cdk5 was down-regulated (Fig. 4*D*, lanes 1 and 4, top panel). Interestingly, we also noticed that STAT3 serine phosphorylation was reduced upon genotoxic treatment in the absence of the kinase (Fig. 4*D*, compare lanes 3 and 4, middle panel). Note, however, that we were not able to completely down-regulate STAT3 phosphorylation, suggesting either that the S727-phosphorylated form of STAT3 has an increased half-life or that other kinases are also phosphorylating STAT3. To further confirm that cdk5 was able to phosphorylate STAT3, the kinase was immunoprecipitated from sn38-treated cells and incubated *in vitro* in the presence of cold ATP and a purified preparation of STAT3 Δ 1–716. Western blot analysis confirmed that the transcription factor was effectively phosphorylated on its serine 727 residue under these conditions (Fig. 4*D*, lanes 5 and 6). In addition, we also determined if cdk5 was involved in STAT3 phosphorylation in other experimental conditions. To this end, cells were transfected with siRNA as described above, serum-starved, and then stimulated with IL-6 for 30 min. Results indicates that cdk5 was not involved in the activation of STAT3 by this cytokine (Fig. 4*D*, lanes 7–9).

It is well known that STAT3 is present in the cytoplasm and in the nucleus. In addition, it has also been reported that cdk5 is localized in the cytoplasm to regulate the neuronal architecture. To determine the localization of these proteins following topoisomerase I inhibition, fractionation experiments have been performed (Fig. 4*E*, lanes 1–12). Results showed that both STAT3 and cdk5 were present in the nucleus and on the chromatin following sn38 treatment (Fig. 4*E*, lanes 6, 7, and 12). As observed in Fig. 1, STAT3 phosphorylation was maximal at 72 h. Both proteins were also activated in the cytoplasm; however, cdk5 activation occurred first in the nucleus, suggesting that the initial activation event might occur in this compartment between 24 and 48 h. Interestingly, we were also able to detect cdk5 on chromatin but only its non-phosphorylated form. However, ChIP experiments indicated that cdk5 was not associated with STAT3 on its target genes (see below). These fractionation experiments also indicated that p35 was not present in the nucleus. Because p35 and cdk5 interact, we then asked whether p35 binds to STAT3 in response to sn38. As described above, total cell extracts were recovered, and immunoprecipitations were performed with polyclonal antibodies directed either against p35 or nonspecific antibodies (Fig. 4*E*,

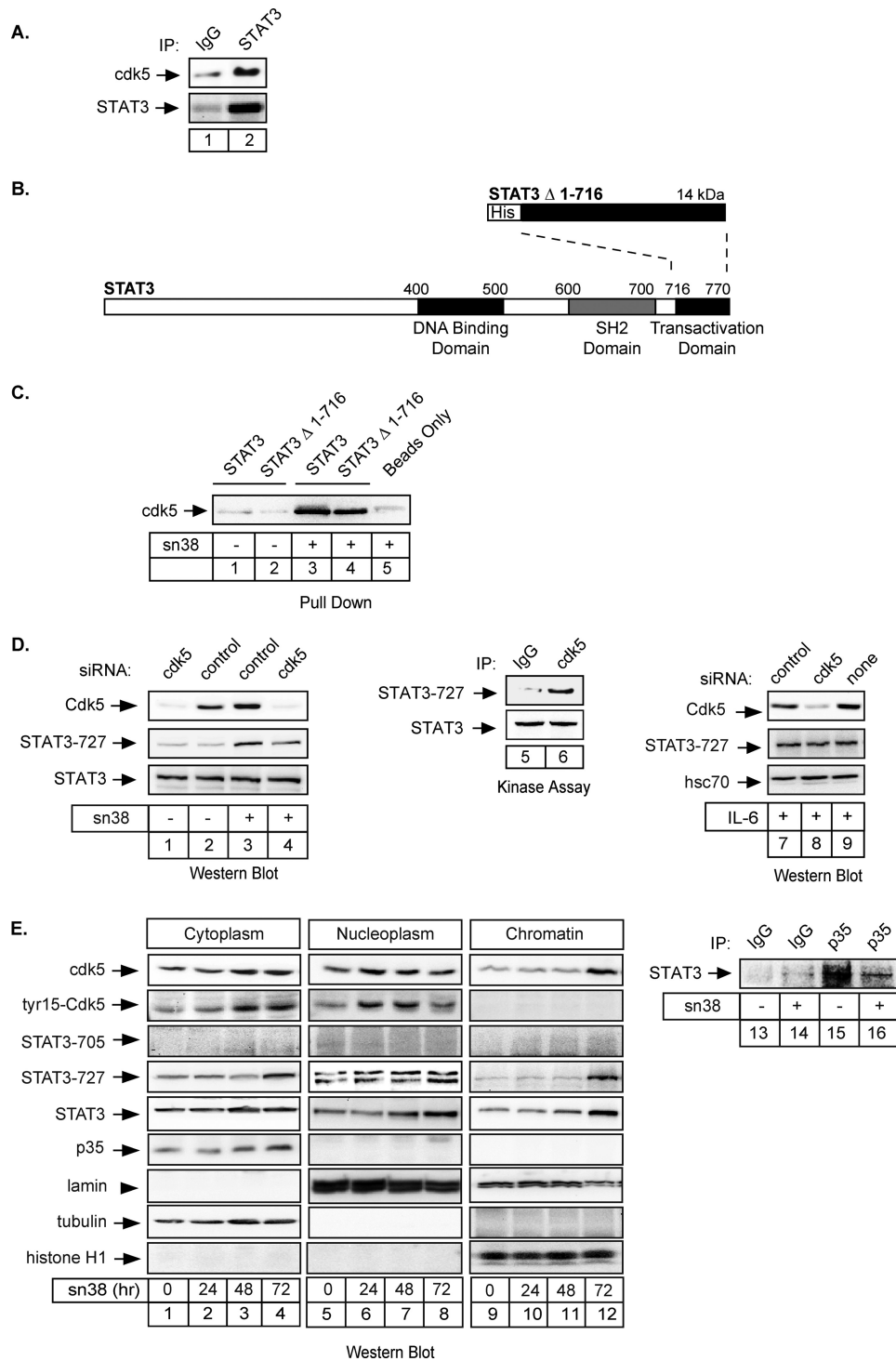


FIGURE 4. Cdk5 interacts with STAT3 to induce its phosphorylation on Serine 727. *A*, HT29 cells were treated with sn38 for 48 h, and whole cell extracts were then immunoprecipitated with polyclonal antibodies directed against STAT3 proteins (*lane 2*) or a control serum (*lane 1*), separated by SDS-PAGE, transferred to a nitrocellulose filter, and probed with polyclonal antibodies directed against STAT3 or cdk5 proteins as indicated. *B*, representation of the fusion proteins used in the pull-down experiments. *C*, total cell extracts (300 μ g) were incubated with histidine, with His-tagged STAT3Cter (STAT3 Δ 1-716), or with the full-length STAT3 (his-STAT3) immobilized on nickel-agarose beads (400 ng). Samples were then separated on polyacrylamide gels, and cdk5 binding was detected by Western blot using anti-cdk5 polyclonal antibodies (*lanes 1-4*). *D*, growing HT29 cells were either transfected with cdk5-specific siRNA oligonucleotides or control oligonucleotides as indicated. Cdk5 expression and phosphorylation of STAT3 on its serine residue were monitored after treatment with sn38 for 48 h (*lanes 1-4*, $n = 4$). In parallel, cdk5 was immunoprecipitated from sn38-treated cells and incubated with STAT3 Δ 1-716 for 10 min at RT in the presence of cold ATP. The phosphorylation of STAT3 on its serine 727 residue was analyzed by Western blot as described above (*lanes 5 and 6*). In parallel, growing HT29 cells were either transfected with cdk5-specific siRNA or control siRNA as indicated, serum-starved, and then stimulated with IL-6 for 30 min. Cdk5 expression and STAT3 phosphorylation were monitored as above ($n = 2$). *E*, HT29 cells were treated with sn38 for the indicated times and cytoplasmic, nuclear, or chromatin extracts were prepared and analyzed by Western blot analysis using antibodies directed against the indicated proteins ($n = 2$, *lanes 1-12*). Lamin, tubulin, and histone expression were used as loading controls for each compartment. In parallel, HT29 cells were treated or not with sn38 for 48 h, and whole cell extracts were then immunoprecipitated with polyclonal antibodies directed against p35 (*lanes 15 and 16*) or a control serum (*lanes 13 and 14*), separated by SDS-PAGE, transferred to a nitrocellulose filter, and probed with polyclonal antibodies directed against STAT3 proteins as indicated.

The *cdk5*-STAT3-*Eme1* Pathway Prevents DNA Damage

lanes 13–16). Proteins present in the immunoprecipitates were revealed by immunoblotting with the reciprocal STAT3 antibodies. Under these conditions, STAT3 was found to co-immunoprecipitate with p35. Interestingly, this association was inhibited following sn38 treatment (Fig. 4E, compare lanes 15 and 16). This was expected if these proteins localized in two different compartments following topoisomerase I inhibition. Taken together, these results suggest that *cdk5* binds to STAT3 upon topoisomerase I inhibition to induce its phosphorylation on serine 727.

The *cdk5* Kinase Regulates the Activation of STAT3 Target Genes following Topoisomerase I Inhibition—We then wanted to determine if *cdk5* is involved in the regulation of STAT3 target genes following sn38 treatment. It is well known that STAT3 regulates the expression of cyclin D1 in growing cells to induce cell cycle progression (36). Because sn38 treatment induced growth inhibition (see Fig. 2), we then determined if topoisomerase I inhibition prevented cyclin D1 expression and if this was linked to *cdk5* activation. To this end, cells were treated or not with sn38, and the expression of the cyclin was evaluated by quantitative RT-PCR and Western blot experiments. As expected, results indicated that genotoxic treatment down-regulated the expression of the cyclin D1 mRNA and protein (Fig. 5A). STAT3 was phosphorylated as expected on the serine 727 under these conditions. To determine if STAT3 is associated with the cyclin D1 promoter and if this binding is regulated in response to SN38, ChIP experiments were then performed using STAT3 antibodies and primers encompassing the proximal promoter where a binding site for the transcription factor has been recently described (37). Antibodies directed against the Ras protein were used as negative controls. As previously shown, ChIP experiments confirmed that STAT3 was present on the proximal cyclin D1 promoter in growing cells. Importantly, the association of the transcription factor with DNA was significantly inhibited following sn38 treatment (Fig. 5B, lanes 5 and 6). As a control, PCR analysis did not detect any occupancy of the $-2760/-2486$ region of the *p21^{waf1}* gene by STAT3 (data not shown). The ChIP result was obtained by semi-quantitative PCR (Fig. 5B, compare lanes 5 and 6) and quantified by quantitative-PCR (Fig. 5B, lanes 7 and 8). We then determined if *cdk5* was involved in the inhibition of the *cyclin D1* gene upon sn38 treatment. As described above, cells were transfected with a pool of three siRNA directed against *cdk5* or the corresponding control siRNA, and the expression of cyclin D1 was then investigated following sn38 treatment by quantitative RT-PCR analysis. As expected, genotoxic treatment reduced the expression of the cyclin D1 mRNA, and the same effect was observed when cells were transfected with control siRNA (Fig. 4C). Interestingly, the sn38-mediated inhibition of cyclin D1 was not observed anymore in the absence of *cdk5*.

Besides cyclin D1, we and others have also shown that the Myc-cdc25a pathway is also an important target of the STAT3 oncogene (38–41). To extend our results, we therefore determined if *cdk5* was involved in the regulation of the *myc* gene upon genotoxic treatment. As expected, ChIP experiments indicated that STAT3 was associated with the proximal promoter of the *myc* gene in growing HT29 cells (Fig. 5D, compare

lanes 3 and 5). As described above for the *cyclin D1* gene, the association of the transcription factor with the *myc* promoter was significantly inhibited following sn38 treatment (Fig. 5D, lanes 5 and 6). The expression of the Myc mRNA was then investigated following sn38 treatment and transfection with a pool of three siRNA directed against *cdk5* or with the corresponding controls. As previously shown (23, 28), Myc expression was down-regulated following topoisomerase I inhibition. Interestingly, results showed that this inhibition was reduced in the absence of *cdk5* (Fig. 5D, right panel). Although this does not rule out the participation of others regulators, these results suggest that *cdk5* also regulates the STAT3-mediated activation of *myc* following DNA damage.

To further extend this observation, we then determined if *cdk5* was only involved in the regulation of proliferative genes such as *cyclin D1* or *myc*, or if its effects could also be observed on other genes regulated by STAT3. We have recently shown that STAT3 can bind to the promoter of the *Eme1* gene to induce its expression (24). *Eme1* is an endonuclease that is implicated in the rescue of broken replication forks in response to topoisomerase I inhibition (42–44). Using quantitative PCR analysis, we confirmed in HT29 cells that *Eme1* expression was increased in response to sn38 (Fig. 6A, lanes 1 and 2). In addition, ChIP experiments also indicated that STAT3 effectively bound to the *Eme1* promoter following DNA damage (Fig. 6A, lanes 5 and 6). To determine if *cdk5* was involved in the activation of the endonuclease, its expression was then investigated in the presence or absence of siRNA directed against the kinase. As expected, *Eme1* expression was increased in the presence of control siRNA in response to sn38 (Fig. 6A, right part). However, when cells were transfected with a pool of three siRNAs directed against *cdk5*, the sn38-mediated expression of the endonuclease was significantly reduced (Fig. 6A, right part). The expression of *Eme1* has been correlated with DNA damage, chromosomal aberrations, and genetic stability. Based on these observations, we made the hypothesis that the down-regulation of *cdk5* or STAT3 might potentiate the effect of sn38 on DNA damage through a reduced expression of the endonuclease. To this end, cells were transfected with pools of three siRNA directed against STAT3 or *cdk5*, treated or not with sn38, and DNA damage was investigated by FACS analysis using an antibody directed against the Ser-139-phosphorylated form of histone H2Ax. Results presented Fig. 6B show as expected that topoisomerase I inhibition induced a significant increase in H2Ax phosphorylation (compare the first and second panel). Interestingly, we also observed that DNA damage was enhanced in the absence of *cdk5* or STAT3 (compare the second panel with panels 3 and 4). FACS quantification (Fig. 6C) confirmed that the percentage of cells with increased DNA damage is higher in the absence of STAT3 or *cdk5*.

To further extend this result, we then determined if *cdk5* down-regulation enhanced cell death following topoisomerase I inhibition. This would be expected as a consequence of increased DNA damage. To this end, cells were transfected with control siRNA or a pool of siRNAs directed against *cdk5* for 2 days, and cells were then split and treated for 10–14 days with sn38. Results from clonogenic assays presented in Fig. 6D showed that *cdk5* down-regulation resulted in a significant

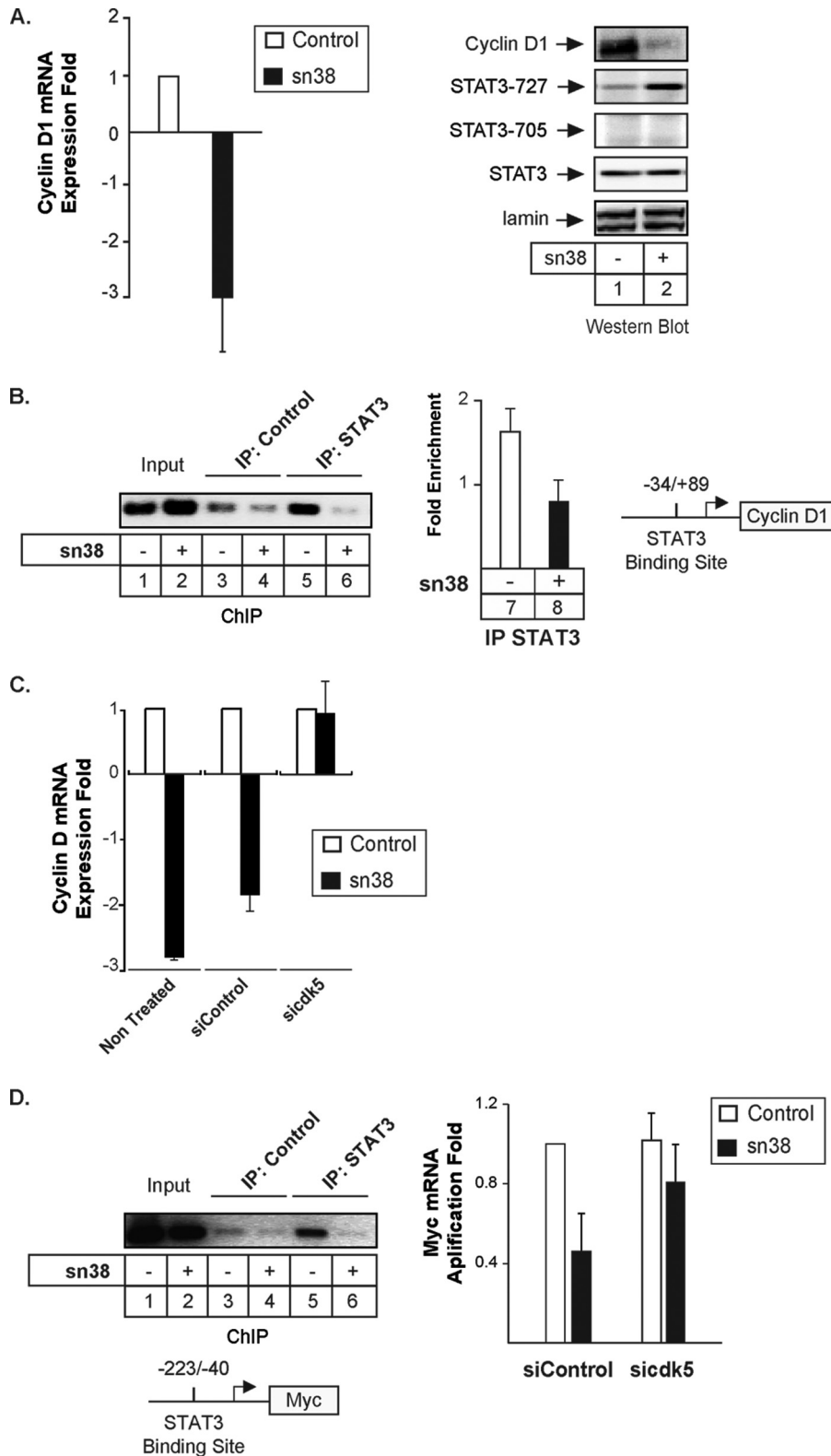


FIGURE 5. **Cdk5 is involved in the down-regulation of cyclin D1 and myc following topoisomerase I inhibition.** *A*, growing HT29 cells were incubated with sn38 (5 ng/ml) for 48 h, and the expression of the cyclin D1 mRNA was analyzed by quantitative RT-PCR experiments ($n = 3$). In parallel, Western blot experiments were also performed to confirm the down-regulation of the cyclin D1 protein and the phosphorylation of STAT3 on its serine residue (*lanes 1* and *2*). *B*, HT29 growing cells were treated as described above, and soluble chromatin was prepared from the indicated cells and immunoprecipitated with antibodies directed against STAT3 or control antibodies. DNA was amplified using one pair of primers that covers the STAT3 proximal binding site of the cyclin D1 promoter. ChIP assays were analyzed on agarose gel (*left part*) or quantified by real-time PCR ($n = 3$, *right part* of the figure). *C*, growing HT29 cells were left untreated or transfected with *cdk5*-specific or control siRNA oligonucleotides as indicated. Cyclin D1 mRNA expression was analyzed by quantitative RT-PCR experiments following sn38 treatment ($n = 3$). *D*, growing HT29 cells were treated as described above, and the association of STAT3 with the myc proximal promoter was analyzed by ChIP (*lanes 1–6*). In parallel, myc expression was evaluated by quantitative RT-PCR in the presence or absence of *cdk5* (*right part*, $n = 4 \pm$ S.D.).

The *cdk5*-STAT3-*Eme1* Pathway Prevents DNA Damage

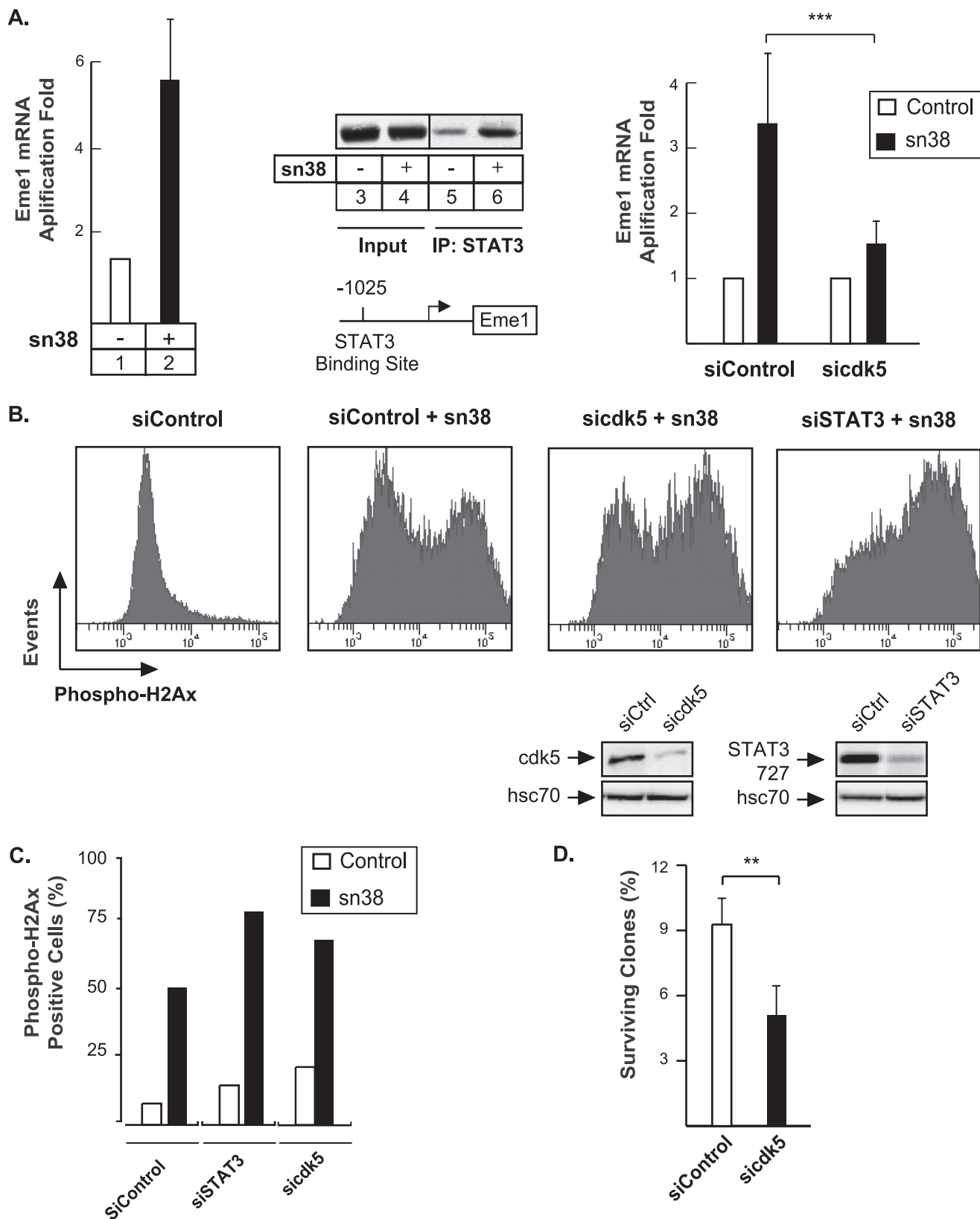


FIGURE 6. The *cdk5*-STAT3 pathway regulates the expression of *Eme1* and reduces DNA damage. *A*, *Eme1* mRNA expression was analyzed by quantitative RT-PCR (*lanes 1 and 2*), and STAT3 association with the *Eme1* promoter was characterized by ChIP (*lanes 3–6*) following sn38 treatment. In parallel, cells were transfected with control or *cdk5* siRNA and then treated with sn38 (5 ng/ml) for 48 h. The expression of the *Eme1* mRNA was analyzed by RT-QPCR experiments ($n = 3 \pm$ S.D., $p < 0.001$). *B* and *C*, growing HT29 cells were transfected with specific or control siRNA and treated or not with sn38 (5 ng/ml). The generation of DNA double strand breaks was quantified by FACS analysis using polyclonal antibodies directed against the ser 139 phosphorylated form of histone H2Ax (one experiment representative of three). *D*, HT29 cells were transfected with pools of siRNAs directed against *cdk5* or control siRNAs for 48 h. Cells were then split and treated with sn38 for 10–14 days. The percentage of colony-forming cells was evaluated as compared with non-treated cells ($n = 3 \pm$ S.D., $p < 0.01$).

decrease of cell viability as compared with control cells. Altogether, these results suggest that *cdk5* interacts with STAT3 to regulate the expression of *Eme1* and that this allows DNA repair in response to topoisomerase I inhibition.

STAT3 Is Associated with the Eme1 Promoter, Phosphorylated on Serine 727, but Not on Tyrosine 705—These results suggest that STAT3 can function as a transcriptional regulator following serine 727 phosphorylation, in the absence of tyrosine 705 phosphorylation. To test this hypothesis, ChIP experiments were performed in HT29 cells using antibodies directed against either the tyrosine (Tyr-705), the serine (Ser-727) phosphorylated forms of the transcription factor or one polyclonal antibody directed against all forms of STAT3 (Fig. 7). Two conditions have been used, growing cells treated or not with sn38 for the indicated times, or cells that have been serum-starved and stimulated with IL-6 for 30 min. DNA binding has been characterized on the *Eme1*, *cyclin D1*, and *Myc* promoters. We observed as expected that STAT3 was recruited to the *Eme1* gene following sn38 treatment (Fig. 7A, lanes 1–3). Interestingly, the same recruitment was noticed using the Ser-727 antibody, but the Tyr-705 antibody did not detect any STAT3 binding (Fig. 7, lanes 4–9). This observation further suggests that a serine-phosphorylated form of STAT3 can be found associated with a target gene in the absence of tyrosine phosphorylation. When cells were stimulated with IL-6 (Fig. 7B), STAT3 was not recruited to the *Eme1* gene, indicating that this promoter is not a target of the transcription following cytokine stimulation. On the *cyclin D1* and *Myc* promoters (Fig. 7, C and D), results showed that STAT3 was present on both promoters in growing cells and that its binding was inhibited following sn38 treatment. This was observed using either a “total” antibody or an antibody directed against the tyrosine-phosphorylated form of the transcription factor (Fig. 7, C and D, lanes 1–2 and 5–6). In serum-starved cells, STAT3 was not present on these promoters, but the transcription factor was recruited following IL-6 stimulation. As expected, this promoter-associated form was phosphorylated on tyrosine 705 (Fig. 7, C and D, lanes 7–8 and 11–12). This observation corresponds to results that have been published previously by our group and others, showing that STAT3 can activate the *myc* and *cyclin D1* genes following JAK-mediated phosphorylation of tyrosine 705 and the recruitment of transcriptional activators such as CBP, SRC, or P/Tefb. Interestingly, we were not able to detect a significant recruitment of STAT3 phosphorylated on its serine residue on these two promoters. Note, however, that this site may not be accessible when the dimer is bound to DNA, whereas this would be the case following DNA damage if STAT3 has a different conformation or different partners. Taken together, these results indicate that STAT3 can be found associated with the *Eme1* promoter in response to DNA damage when phosphorylated only on its serine 727 residue.

DISCUSSION

In this study, we have found that the STAT3 transcription factor is phosphorylated on its serine C-terminal residue but not on tyrosine 705 upon topoisomerase I inhibition. Our results indicate that this is due to the activation of the *cdk5* kinase, which binds to the C-terminal of domain of the tran-

scription factor to induce its phosphorylation. Importantly, *cdk5* is involved in the down-regulation of early G_1 genes such as *myc* and *cyclin D1* and in the STAT3-mediated up-regulation of the *Eme1* gene, an endonuclease involved in the processing of damaged replication forks. In light of these results, we propose that the *cdk5-STAT3-Eme1* pathway plays an important role in the response to topoisomerase I inhibition and chemotherapy treatments.

It is well known that STAT3 is activated at the G_0 - G_1 transition following cytokine or growth factor stimulation. In this condition, the transcription factor binds to the promoter of several cell cycle genes such as *myc*, *cyclin D1*, *fos*, or *cdc25A* to induce their expression and activate progression toward S phase. Gene activation by STAT3 during the G_0 - G_1 transition is due to the phosphorylation of STAT3 on its tyrosine residue, followed by nuclear translocation and DNA binding. The second phosphorylation of STAT3 on its serine residue allows the contact of the tyrosine-phosphorylated dimer with transcriptional cofactors such as CBP, NcoA, or Ptefb. However, this pathway is probably not the only mechanism by which STAT proteins are activated, because several results have shown that these transcription factors induce transcription in the absence of tyrosine phosphorylation. This was originally described with STAT1 when it was shown that this transcription factor can drive the expression of several genes in the absence of tyrosine phosphorylation (45). Using non-phosphorylated forms of STAT3 on its tyrosine residue, Yang *et al.* have shown that these mutants can induce the expression of genes such as *met* and *mras*, which certainly play an important role in the oncogenic activity of STAT3. Under these conditions, gene activation is a consequence of the formation of a STAT3-NF- κ B enhanceosome that plays a key role in transformed cells (12, 13). Most importantly, the genes regulated by STAT3 in these conditions are normally not activated when the transcription factor is phosphorylated on its tyrosine residue. This leads to the important conclusion that the STAT3 transcriptional targets depends on its post-translational modifications.

Importantly, using ChIP analysis, we have been able to detect STAT3 on the *Eme1* promoter when phosphorylated only on its Ser-727 residue. We therefore propose that STAT3 is activated by DNA damage during the G_2 phase of the cell cycle and that its serine phosphorylation allows the specific up-regulation of DNA repair genes such as the *Eme1* endonuclease. Surprisingly, the role of STAT3 in the response to genotoxic treatment has not been well characterized. By contrast, it is known that both STAT1 and STAT5 are regulated following DNA damage. STAT1 is involved in the S and G_2 /M checkpoints and can associate with repair signaling proteins such as Chk2 and Mdc1 in response to γ -irradiation (46, 47). In addition, this transcription factor is also phosphorylated in response to topoisomerase inhibitors (47). STAT5 has been shown to regulate the expression of *rad51* and, importantly, this has been linked to the ability of several oncogenic kinases such as *bcr-abl* or *tel-jak2* to induce drug resistance (48, 49). Interestingly, recent results also suggest that STAT3 plays an important role in the regulation of genome stability. The inactivation of the T-cell protein tyrosine phosphatase induces a constitutive activation of STAT3 probably as a consequence of replication fork stall-

The *cdk5*-STAT3-*Eme1* Pathway Prevents DNA Damage

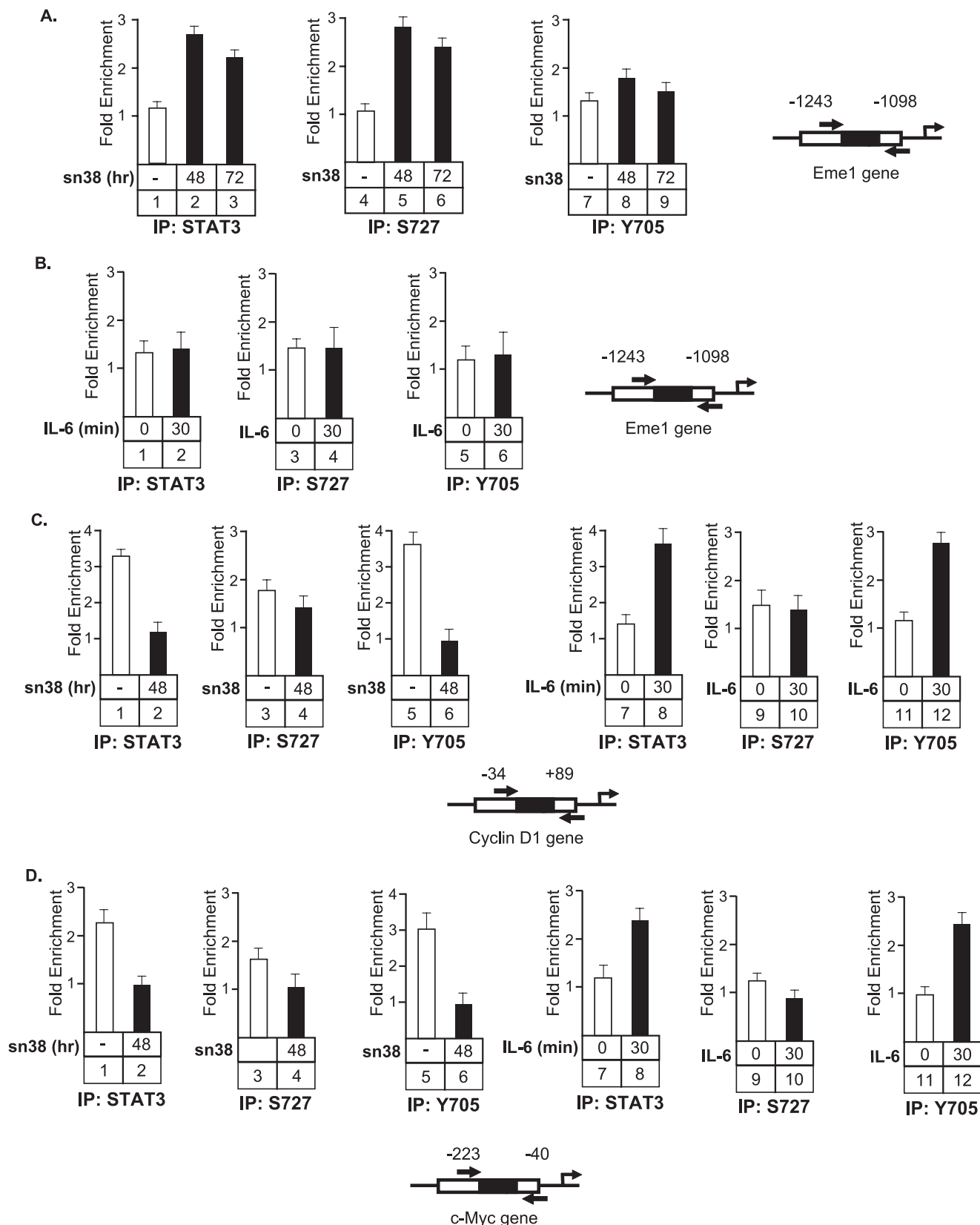


FIGURE 7. STAT3 is recruited to the *Eme1* promoter when phosphorylated only on its serine 727 residue. Growing HT29 cells were treated or not with sn38 as indicated above and soluble chromatin was prepared and immunoprecipitated with antibodies directed against STAT3 (*IP:STAT3*) or its serine or tyrosine phosphorylated forms (*IP:S727* or *IP:Y705*). In parallel, cells were serum-starved and stimulated or not with IL-6 (10 ng/ml) for 30 min, and the chromatin was immunoprecipitated under the same conditions. DNA was amplified using pair of primers that covers the STAT3 proximal binding sites of the cyclin D1 (*panel C*), *Myc* (*panel D*), and *Eme1*, (*panel A and B*) promoters as indicated. ChIP assays were then quantified by real-time PCR as compared with the signals obtained on each genes with a control IgG ($n = 3$). Note that sn38 (-) in the legend means growing cells, whereas *IL6* (0) means serum-starved cells.

ing, and this leads to aberrant mitoses with lagging chromosomes (50). Unfortunately, the link between STAT3 and DNA repair has not been characterized in this study, because this effect has been linked to a sustained expression of cyclin D1 during S phase. Further suggesting a link between STAT3 and DNA stability, it is well known that a direct target of STAT3, myc, can induce DNA damage and dysregulate genomic stability and DNA repair pathways (51). In this study, we further extend these observations, showing that this transcription factor is activated by Cdk5 in response to topoisomerase I inhibitors. We speculate that this kinase allows the formation of a new STAT3 enhanceosome that would specifically regulate the expression of DNA repair genes upon genotoxic treatment. In light of recent results showing an essential role of NF- κ B in the response to DNA damage (52), one interesting hypothesis is that genes involved in the response to sn38 are controlled by a specific STAT3-NF- κ B complex that would be activated by cdk5. It will be interesting to determine if this enhanceosome preferentially binds DNA repair genes as opposed to more conventional STAT3 targets such as myc or cdc25A.

As a consequence of DNA repair genes regulation, our results indicate that the cdk5-STAT3 pathway reduces DNA damage in response to topoisomerase I inhibition. This suggests that these proteins might play an essential role in the resistance of cancer cells to chemotherapy. Further confirming the importance of this oncogenic cascade, recent results have shown that the cdk5-STAT3 pathway plays an essential role in thyroid carcinomas (53). In addition, we and others have recently shown that STAT3 prevents the induction of senescence through p53-p21 inactivation (18, 40, 54, 55). Interestingly, cdk5 is also involved in senescence programs, because this kinase regulates cell morphology through ezrin and rac1 modulation (32, 33). It will be interesting to determine if cdk5 is also involved in the inactivation of the p53-p21 pathway by the STAT3 oncogene during senescence induction.

In light of this study and other results (53), we therefore propose that cdk5 plays an important role in cell transformation by the STAT3 oncogene. Because it has been proposed that cell transformation induces an intrinsic resistance program to chemotherapy (56), we speculate that cdk5-STAT3 provides cancer cells with intrinsic resistance capacities due to enhanced Eme1 expression and that this a corollary of cell transformation. We propose that the early detection on tumor biopsies of the cdk5-STAT3 oncogenic pathway, both of its phosphorylation status and of its target genes, will provide oncologists with a resistance profile indicative of tumors that will fail to respond to chemotherapy (15, 57). In addition, we also propose that STAT3 inhibitors, which are emerging as new targeted cancer therapies (2, 57, 58) should be tested in clinical trials in combination with irinotecan to reduce DNA repair and enhance the efficiency of genotoxic treatments.

REFERENCES

- Bromberg, J. (2002) *J. Clin. Invest.* **109**, 1139–1142
- Yu, H., and Jove, R. (2004) *Nat. Rev. Cancer* **4**, 97–105
- Levy, D. E., and Lee, C. K. (2002) *J. Clin. Invest.* **109**, 1143–1148
- Bromberg, J. F., Horvath, C. M., Besser, D., Lathem, W. W., and Darnell, J. E., Jr. (1998) *Mol. Cell. Biol.* **18**, 2553–2558
- Bromberg, J. F., Wrzeszczynska, M. H., Devgan, G., Zhao, Y., Pestell, R. G., Albanese, C., and Darnell, J. E., Jr. (1999) *Cell* **98**, 295–303
- Wen, Z., Zhong, Z., and Darnell, J. E., Jr. (1995) *Cell* **82**, 241–250
- Giraud, S., Bienvendu, F., Avril, S., Gascan, H., Heery, D. M., and Coqueret, O. (2002) *J. Biol. Chem.* **277**, 8004–8011
- Giraud, S., Hurlstone, A., Avril, S., and Coqueret, O. (2004) *Oncogene* **23**, 7391–7398
- Paulson, M., Pisharody, S., Pan, L., Guadagno, S., Mui, A. L., and Levy, D. E. (1999) *J. Biol. Chem.* **274**, 25343–25349
- Nakashima, K., Yanagisawa, M., Arakawa, H., Kimura, N., Hisatsune, T., Kawabata, M., Miyazono, K., and Taga, T. (1999) *Science* **284**, 479–482
- Qin, H. R., Kim, H. J., Kim, J. Y., Hurt, E. M., Klarmann, G. J., Kawasaki, B. T., Duhagon Serrat, M. A., and Farrar, W. L. (2008) *Cancer Res.* **68**, 7736–7741
- Yang, J., Chatterjee-Kishore, M., Staugaitis, S. M., Nguyen, H., Schlessinger, K., Levy, D. E., and Stark, G. R. (2005) *Cancer Res.* **65**, 939–947
- Yang, J., Liao, X., Agarwal, M. K., Barnes, L., Auron, P. E., and Stark, G. R. (2007) *Genes Dev.* **21**, 1396–1408
- Lee, H., Herrmann, A., Deng, J. H., Kujawski, M., Niu, G., Li, Z., Forman, S., Jove, R., Pardoll, D. M., and Yu, H. (2009) *Cancer Cell* **15**, 283–293
- Barré, B., Vigneron, A., Perkins, N., Roninson, I. B., Gamelin, E., and Coqueret, O. (2007) *Trends Mol. Med.* **13**, 4–11
- Sano, S., Chan, K. S., Kira, M., Kataoka, K., Takagi, S., Tarutani, M., Itami, S., Kiguchi, K., Yokoi, M., Sugasawa, K., Mori, T., Hanaoka, F., Takeda, J., and DiGiovanni, J. (2005) *Cancer Res.* **65**, 5720–5729
- Shen, Y., Devgan, G., Darnell, J. E., Jr., and Bromberg, J. F. (2001) *Proc. Natl. Acad. Sci. U.S.A.* **98**, 1543–1548
- Niu, G., Wright, K. L., Ma, Y., Wright, G. M., Huang, M., Irby, R., Briggs, J., Karras, J., Cress, W. D., Pardoll, D., Jove, R., Chen, J., and Yu, H. (2005) *Mol. Cell. Biol.* **25**, 7432–7440
- Catlett-Falcone, R., Landowski, T. H., Oshiro, M. M., Turkson, J., Levitzki, A., Savino, R., Ciliberto, G., Moscinski, L., Fernández-Luna, J. L., Nuñez, G., Dalton, W. S., and Jove, R. (1999) *Immunity* **10**, 105–115
- Duan, Z., Foster, R., Bell, D. A., Mahoney, J., Wolak, K., Vaidya, A., Hampel, C., Lee, H., and Seiden, M. V. (2006) *Clin. Cancer Res.* **12**, 5055–5063
- Diaz, N., Minton, S., Cox, C., Bowman, T., Gritsko, T., Garcia, R., Eweis, I., Wloch, M., Livingston, S., Seijo, E., Cantor, A., Lee, J. H., Beam, C. A., Sullivan, D., Jove, R., and Muro-Cacho, C. A. (2006) *Clin. Cancer Res.* **12**, 20–28
- Gritsko, T., Williams, A., Turkson, J., Kaneko, S., Bowman, T., Huang, M., Nam, S., Eweis, I., Diaz, N., Sullivan, D., Yoder, S., Enkemann, S., Eschrich, S., Lee, J. H., Beam, C. A., Cheng, J., Minton, S., Muro-Cacho, C. A., and Jove, R. (2006) *Clin. Cancer Res.* **12**, 11–19
- Vigneron, A., Roninson, I. B., Gamelin, E., and Coqueret, O. (2005) *Cancer Res.* **65**, 8927–8935
- Vigneron, A., Gamelin, E., and Coqueret, O. (2008) *Cancer Res.* **68**, 815–825
- Dhavan, R., and Tsai, L. H. (2001) *Nat. Rev. Mol. Cell Biol.* **2**, 749–759
- Gong, X., Tang, X., Wiedmann, M., Wang, X., Peng, J., Zheng, D., Blair, L. A., Marshall, J., and Mao, Z. (2003) *Neuron* **38**, 33–46
- Wang, C. X., Song, J. H., Song, D. K., Yong, V. W., Shuaib, A., and Hao, C. (2006) *Cell Death Differ.* **13**, 1203–1212
- Vigneron, A., Cherier, J., Barré, B., Gamelin, E., and Coqueret, O. (2006) *J. Biol. Chem.* **281**, 34742–34750
- Le, H. V., Minn, A. J., and Massagué, J. (2005) *J. Biol. Chem.* **280**, 32018–32025
- Turner, N. C., Lord, C. J., Iorns, E., Brough, R., Swift, S., Elliott, R., Rayter, S., Tutt, A. N., and Ashworth, A. (2008) *EMBO J.* **27**, 1368–1377
- Tian, B., Yang, Q., and Mao, Z. (2009) *Nat. Cell Biol.* **11**, 211–218
- Alexander, K., Yang, H. S., and Hinds, P. W. (2004) *Mol. Cell. Biol.* **24**, 2808–2819
- Yang, H. S., and Hinds, P. W. (2003) *Mol. Cell* **11**, 1163–1176
- Fu, A. K., Fu, W. Y., Ng, A. K., Chien, W. W., Ng, Y. P., Wang, J. H., and Ip, N. Y. (2004) *Proc. Natl. Acad. Sci. U.S.A.* **101**, 6728–6733
- Lee, J. H., Jeong, M. W., Kim, W., Choi, Y. H., and Kim, K. T. (2008) *J. Biol. Chem.* **283**, 19826–19835
- Leslie, K., Lang, C., Devgan, G., Azare, J., Berishaj, M., Gerald, W., Kim, Y. B., Paz, K., Darnell, J. E., Albanese, C., Sakamaki, T., Pestell, R., and Bromberg, J. (2006) *Cancer Res.* **66**, 2544–2552

The *cdk5-STAT3-Eme1* Pathway Prevents DNA Damage

37. Lo, H. W., Hsu, S. C., Ali-Seyed, M., Gunduz, M., Xia, W., Wei, Y., Bartholomeusz, G., Shih, J. Y., and Hung, M. C. (2005) *Cancer Cell* **7**, 575–589
38. Kiuchi, N., Nakajima, K., Ichiba, M., Fukada, T., Narimatsu, M., Mizuno, K., Hibi, M., and Hirano, T. (1999) *J. Exp. Med.* **189**, 63–73
39. Bowman, T., Broome, M. A., Sinibaldi, D., Wharton, W., Pledger, W. J., Sedivy, J. M., Irby, R., Yeatman, T., Courtneidge, S. A., and Jove, R. (2001) *Proc. Natl. Acad. Sci. U.S.A.* **98**, 7319–7324
40. Barré, B., Avril, S., and Coqueret, O. (2003) *J. Biol. Chem.* **278**, 2990–2996
41. Barré, B., Vigneron, A., and Coqueret, O. (2005) *J. Biol. Chem.* **280**, 15673–15681
42. Dendouga, N., Gao, H., Moechars, D., Janicot, M., Vialard, J., and McGowan, C. H. (2005) *Mol. Cell. Biol.* **25**, 7569–7579
43. Osman, F., and Whitby, M. C. (2007) *DNA Repair* **6**, 1004–1017
44. Pommier, Y., Redon, C., Rao, V. A., Seiler, J. A., Sordet, O., Takemura, H., Antony, S., Meng, L., Liao, Z., Kohlhagen, G., Zhang, H., and Kohn, K. W. (2003) *Mutat. Res.* **532**, 173–203
45. Chatterjee-Kishore, M., Wright, K. L., Ting, J. P., and Stark, G. R. (2000) *EMBO J.* **19**, 4111–4122
46. Townsend, P. A., Cragg, M. S., Davidson, S. M., McCormick, J., Barry, S., Lawrence, K. M., Knight, R. A., Hubank, M., Chen, P. L., Latchman, D. S., and Stephanou, A. (2005) *J. Cell Sci.* **118**, 1629–1639
47. Thomas, M., Finnegan, C. E., Rogers, K. M., Purcell, J. W., Trimble, A., Johnston, P. G., and Boland, M. P. (2004) *Cancer Res.* **64**, 8357–8364
48. Slupianek, A., Schmutte, C., Tomblin, G., Nieborowska-Skorska, M., Hoser, G., Nowicki, M. O., Pierce, A. J., Fishel, R., and Skorski, T. (2001) *Mol. Cell* **8**, 795–806
49. Slupianek, A., Hoser, G., Majsterek, I., Bronisz, A., Malecki, M., Blasiak, J., Fishel, R., and Skorski, T. (2002) *Mol. Cell. Biol.* **22**, 4189–4201
50. Shields, B. J., Hauser, C., Bukczynska, P. E., Court, N. W., and Tiganis, T. (2008) *Cancer Cell* **14**, 166–179
51. Vafa, O., Wade, M., Kern, S., Beeche, M., Pandita, T. K., Hampton, G. M., and Wahl, G. M. (2002) *Mol. Cell* **9**, 1031–1044
52. Campbell, K. J., Witty, J. M., Rocha, S., and Perkins, N. D. (2006) *Cancer Res.* **66**, 929–935
53. Lin, H., Chen, M. C., Chiu, C. Y., Song, Y. M., and Lin, S. Y. (2007) *J. Biol. Chem.* **282**, 2776–2784
54. Flørenes, V. A., Lu, C., Bhattacharya, N., Rak, J., Sheehan, C., Slingerland, J. M., and Kerbel, R. S. (1999) *Oncogene* **18**, 1023–1032
55. Bienvenu, F., Barre, B., Giraud, S., Avril, S., and Coqueret, O. (2005) *Mol. Biol. Cell* **16**, 1850–1858
56. Johnstone, R. W., Ruefli, A. A., and Lowe, S. W. (2002) *Cell* **108**, 153–164
57. Henderson, B. W., Daroqui, C., Tracy, E., Vaughan, L. A., Loewen, G. M., Cooper, M. T., and Baumann, H. (2007) *Clin. Cancer Res.* **13**, 3156–3163
58. Benekli, M., Baumann, H., and Wetzler, M. (2009) *J. Clin. Oncol.* **27**, 4422–4432